Air Force Institute of Technology
AFIT Scholar

Theses and Dissertations   Student Graduate Works

9-15-2011

Source Normalization Constants for Ground Distributed Fallout Fields

Justin M. Smith

Follow this and additional works at: https://scholar.afit.edu/etd

    Part of the Nuclear Commons

SOURCE NORMALIZATION CONSTANTS FOR GROUND DISTRIBUTED
FALLOUT FIELDS

THESIS

Justin M. Smith, Captain, USAF

AFIT/GNE/ENP/11S02

DEPARTMENT OF THE AIR FORCE
AIR UNIVERSITY

AIR FORCE INSTITUTE OF TECHNOLOGY

Wright-Patterson Air Force Base, Ohio

AFIT/GNE/ENP/11S02

SOURCE NORMALIZATION CONSTANTS FOR GROUND DISTRIBUTED

FALLOUT FIELDS

THESIS

Presented to the Faculty

Department of Engineering Physics

Graduate School of Engineering and Management

Air Force Institute of Technology

Air University

Air Education and Training Command

In Partial Fulfillment of the Requirements for the

Degree of Master of Science in Nuclear Engineering

Justin M. Smith, BS

Captain, USAF

September 2011

AFIT/GNE/ENP/11S02

SOURCE NORMALIZATION CONSTANTS FOR GROUND DISTRIBUTED FALLOUT FIELDS

Justin M. Smith, BS
Captain, USAF

Approved:

_____   _____

Charles J. Bridgman, PhD (Chairman)   Date

_____   _____

Abigail A. Bickley, PhD (Member)   Date

_____   _____

Vincent J. Jodoin, PhD (Member)   Date

Abstract

Five assumptions regarding a first order model developed to calculate dose rate at a detector above a ground distributed fallout field are analyzed. The omission of scattering is relaxed by using an integral method of successive scatters. The assumption of using 0.70MeV as the single average photon energy to represent an entire fallout distribution is analyzed using the Oak Ridge National Laboratory Isotope Generator (ORIGEN) Fallout Analysis Tool provided by Oak Ridge National Laboratory. A normalized Gaussian distribution is used to analyze the effects of non-uniform activity density on the source normalization constant (SNC). The effects of time on the SNC are also examined by the ORIGEN Fallout Analysis Tool in order to determine if a separate time correction factor is needed. Finally, previous research accomplished by Herte regarding self-shielding from terrain roughness is summarized.

Using a weighted average of fallout energy distribution, an average build up factor of 1.1 and an average fallout field photon energy of 0.81MeV is calculated. By comparing these values with a multi-group calculation, they are found to be an accurate approximation of the fallout field and result in a 25% increase to the first order model SNC. The effects of non-uniform activity density are found to be insignificant; however, the effects of time on the SNC are found to warrant an additional time correction factor. In summarizing Herte's results, terrain roughness is shown to produce between 2-5% self-shielding for soil. This value is highly variable depending on the terrain considered, and is not incorporated in the updated SNC value.

Acknowledgments

I would like to express my sincere appreciation to Dr. Charles J. Bridgman for the many hours of instruction, feedback, and insightful guidance during research and preparation of this document. In addition, special thanks to Dr. Vince Jodoin and his team at Oak Ridge National Laboratory for developing the ORIGEN Fallout Analysis Tool, providing instruction, and permitting its instrumental use in this research. I also wish to thank Dr. Abby Bickley for her input regarding error analysis and always having an open door for random questions. Finally, I wish to thank Dr. Kirk Mathews whose sharp eye for eloquent alternative solutions broadened many horizons during this research. As Sir Isaac Newton once said, "If I have seen further it is by standing on the shoulders of giants."

Justin M. Smith

Table of Contents

List of Figures

Figure   Page

List of Tables

SOURCE NORMALIZATION CONSTANTS FOR GROUND DISTRIBUTED

FALLOUT FIELDS

I. Introduction

Perhaps one of the most lingering attributes of a nuclear weapon burst is fallout. Potentially covering vast areas, fallout fields are capable of producing many biological effects ranging from acute radiation syndrome to cancer. Whether conducting a forensic analysis mission or weighing the risks involved with rescue efforts, the dose rate experienced while traversing a fallout field is of paramount concern to all involved.

The fallout from a nuclear weapon burst is distributed across the ground downwind of the burst. The activity density of the fallout is then converted to dose rate through use of the source normalization constant (SNC). An often used approximation of the SNC involves five simplifying assumptions that are analyzed at length in this thesis with the intent to improve the approximate SNC value. This analysis begins with a reproduction of the first order model (FOM) proposed by Bridgman that is used to calculate the current SNC value.

Background

As developed in Chapter 12 of *The Introduction to the Physics of Nuclear Weapons Effects* (Bridgman, 2001:414), consider a detector positioned one meter above a fallout field as depicted in Figure 1.
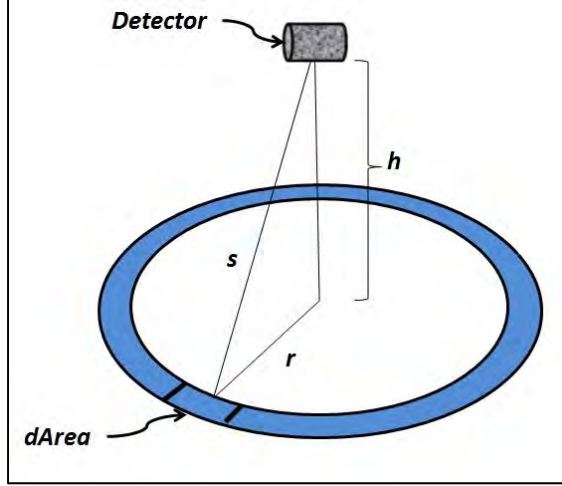
Figure 1. Detector at height _h_ (1m) above a fallout field

The dose rate due to ground distributed gamma ray activity at a given detector position is given by the expression:

$$\dot{D} = \int_{hv=0}^{\infty} \int_{Area} A_{gd}[r,t,hv]\ BUF[hv]\ \frac{e^{-\mu_t[hv]s}}{4\pi s^2}\left(\frac{\mu_a[hv]}{\rho}\right)_{det}(hv)\ dArea\ d(hv)$$

(1)

Where,

$\dot{D}$ is the dose rate in $\left[\dfrac{J}{kg-\sec}\right]$ at the detector ;

$A_{gd}[r,t,hv]$ is the activity density in $\left[\dfrac{Bq}{m^2-J\ of\ the\ \gamma\ spectrum}\right]$ on the ground at a

location r measured from the detector;

$BUF[hv]$ is the energy dependent build up factor due to scattering of gamma rays both

in the air and ground [dimensionless];

s is the slant range from a differential area (_dArea_) to the detector $[m]$;

2

t is time in [sec]

$r = \sqrt{s^2 - 1}$ is the ground distance from a point just under the detector to a differential

area $(dArea)$ in $[m]$;

$\mu_t[hv]$ is the energy dependent macroscopic cross section for attenuation for the

medium through which the gamma rays are traveling $[m^{-1}]$;

$\left[\dfrac{\mu_a[hv]}{\rho}\right]_{det}$ is the energy and material dependent total mass absorption coefficient[1] for

the detector in $\left[\dfrac{m^2}{kg}\right]$;

hv is the energy per disintegration in $[J]$;

$dArea$ is the differential ground area $[m^2]$ and

$d(hv)$ is a differential gamma ray spectrum energy in $[J \ of \ the \ \gamma \ spectrum]$

---

[1] Total mass absorption coefficient includes absorption due to Photoelectric and Compton events

By nature, the gamma ray spectrum of a fallout field is discrete (See Figure 2).
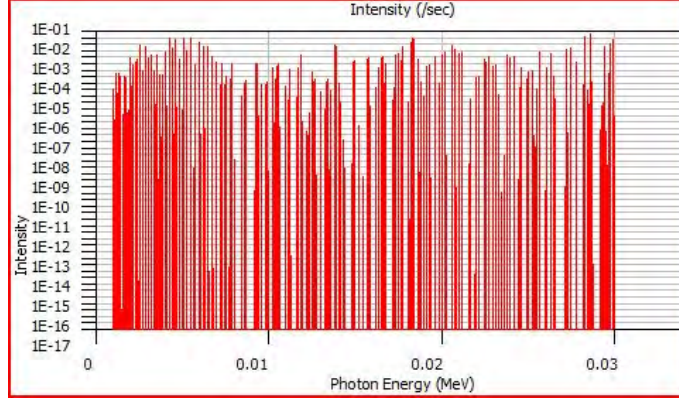
Figure 2. A subset of the gamma ray spectrum for a fallout field generated by the ORIGEN Fallout Analysis Tool for a 1kt 90/10 U-235/U-238 fission at one hour.

This forces the modification of equation (1) by replacing integration across all energies with a discrete summation of all gamma ray energies present at time t.

$$\dot{D}[r,t] = \sum_{g=1}^{G(t)} \int_{Area} \left(A_{gd}[r,t] \right)_g BUF[hv_g] \frac{e^{-\mu_t[hv_g]s}}{4\pi s^2} \left(\frac{\mu_a[hv_g]}{\rho} \right)_{det} (hv)_g dArea \tag{2}$$

Where,

g represents individual gamma ray energies and $G(t)$ the total number of gamma ray energies which varies with time;

hv_g represents the energy of the gamma ray g ;

$\left(A_{gd}[r,t] \right)_g$ is the activity due to gamma rays in group g ;

μ_t and μ_a are the macroscopic cross sections for total attenuation and total absorption

in $\left[m^{-1} \right]$ at the group energy hv_g and

4

BUF is the energy build up factor for gamma rays at energy hv_g.

Simplifying Assumptions

Evaluating equation (2) for all gamma ray energies present at a given time in a fallout field is prohibitively challenging, thus Bridgman makes several simplifying assumptions:

1. He ignores scattering in the ground/air and only calculates the *direct* contribution of gamma rays to the detector.

    a. This implies the build up factor (BUF) is one.

    b. This also implies that any gamma rays directed downward (towards the ground) never return to the detector – meaning he has immediately discounted half of all gamma rays emitted.

2. He replaces the entire discrete spectrum of gamma rays with a single average gamma ray energy of 0.70MeV at a time of one hour.

    a. This eliminates the need to sum across all energy groups as it effectively reduces equation (2) to a one-group calculation.

3. He evaluates activity at one hour and utilizes the Way-Wigner approximation to calculate activity at all other times. Since not all activity may be deposited on the ground at a given time, Bridgman invokes the concept of "unit-time reference" for activity (and inherently dose rate).[2]

4. He assumes the activity density directly under the detector at a position (X, Y) is uniform out to infinity. That is, he assumes that activity density along r does not vary, but instead takes on the value at the foot of the detector.

    a. This also implies that he assumes an unfractionated sample which means the gamma ray spectrum does not vary along r.

    b. Furthermore, the Way-Wigner approximation comes into question for subsets of the total fission product set (volatile/refractory).

5. He assumes the ground is perfectly flat with no surface roughness to impede gamma rays emitted toward the detector.

---

[2] Reference *The Effects of Nuclear Weapons* (Glasstone, 427) for additional information on unit-time reference

The First Order Model

Given an air equivalent detector, these assumptions lay the foundation for a first order model as depicted in the development of the following equations[3]:

$$\dot{D}[X,Y,1] = A[X,Y,1]\left(\frac{\mu_a[hv_{avg}]}{\rho}\right)_{air} (hv)_{avg} \int_0^\infty \frac{e^{-\mu_t[hv_{avg}]_{air}\,s}}{4\pi s^2} 2\pi r dr \tag{3}$$

Since, $s^2 = r^2 + h^2$ equation (3) becomes:

$$\dot{D}[X,Y,1] = A[X,Y,1]\left(\frac{\mu_a[hv_{avg}]}{\rho}\right)_{air} (hv)_{avg} \frac{1}{2}\int_h^\infty \frac{e^{-\mu_t[hv_{avg}]_{air}\,s}}{s} ds \tag{4}$$

Where the integral is recognized as an exponential integral of the first kind:

$$\dot{D}[X,Y,1] = A[X,Y,1]\left(\frac{\mu_a[hv_{avg}]}{\rho}\right)_{air} (hv)_{avg} \frac{1}{2} E_1[\mu_t[hv_{avg}]] \tag{5}$$

Where,

$\dot{D}[X,Y,1]$ is the dose rate at a given location (X,Y) at a time of one hour post

detonation in $\left[\dfrac{J}{kg - \sec}\right]$;

$A[X,Y,1]$ is the activity density at the given location (X,Y) at a time of one hour in

$\left[\dfrac{Bq}{m^2}\right]$ and

E_1 is the exponential integral of the first kind with an argument of μ_t.

---

[3] The equivalent equations in the 2 Aug 2011 revision of *Introduction to the Physics of Nuclear Weapons Effects* (Bridgman) are 12-52a, 12-52b, 12-52c.

If the average gamma ray energy is taken as 0.70 MeV at one hour as suggested by *The Effects of Nuclear Weapons (ENW)* (Glasstone, 1977:454), and if the density of sea level air is taken as 1.23 $\frac{kg}{m^3}$, then the values for equation (5) are:

$$\left(\frac{\mu_a[hv_{avg}]}{\rho}\right)_{air} = 0.0029 \frac{m^2}{kg};$$

$$\mu_t = 0.0092 \ m^{-1} \text{ and}$$

$$E_1[\mu_t] = 4.1$$

The first order model (FOM) then becomes[4]:

$$\dot{D}[X,Y,1] = 6.8 \times 10^{-16} A[X,Y,1] \left\{ \frac{J}{kg - \sec} \right\} \tag{6}$$

The constant, 6.8×10^{-16}, converting activity density at a given location to dose rate is known as the source normalization constant (SNC) in $\left\{ \frac{J - m^2}{kg - \sec - Bq} \right\}$. Traditionally, this value is reported as $2100 \left\{ \frac{R - mi^2}{hr - KT} \right\}$ where activity density is expressed in $\left\{ \frac{KT}{mi^2} \right\}$. In either case, the premise is that dose rate may be obtained through multiplying an activity density by a constant.

Research Objective

The objective of this research is to analyze on the quality of assumptions 1-5. Once this assessment is made, any quantitative impacts will be combined to produce an updated SNC for a ground distributed fallout field at a time of one hour. This analysis begins in Chapter II by examining the impact of the "no scattering" assumption.

---

[4] This value is slightly different from the value of 6.33x10⁻¹⁶ developed by Bridgman due to small differences in the values used for cross section values.

II. The Technique of Successive Scatters

One method for determining the contribution of scattering to the detector is the method of successive scatters (Bridgman, 2001:209). In this technique, the overall scattering contribution is broken up into flights delineated by how many scatters occur between emission and arrival at the detector. For example, the term *first flight* refers to gamma rays that reach the detector without scattering (otherwise known as *direct flight*). Gamma rays scattered once before reaching the detector are referred to as *second flight*, and so on with each progressive flight. Using the *direct flight* contribution as a baseline, each successive flight's contribution is added until the relative contribution from the *n-th flight* falls below an arbitrary error tolerance.

Depending on how many flights are calculated, this technique can become computationally intensive. However, the primary advantage of this integral method is its flexibility with addressing assumptions. More specifically, it continues to be valid as other assumptions are relaxed over the course of this thesis. This makes the technique of successive scatters an ideal choice in relaxing the various assumptions associated with the FOM, beginning with assumption #1: the omission of scattering.

*Note: Scattering is the <u>only</u> assumption relaxed for the following development. All other assumptions for the FOM are in effect unless otherwise annotated.

Direct Flight Contribution

Applied to the fallout field, we begin with the *direct flight* contribution to the detector located at (X,Y) and at a time of one hour. Since this flight accounts for gamma rays that reach the detector without scattering, its development is identical to that of the FOM:

$$\dot{D}[X,Y,1] = A[X,Y,1]\left(\frac{\mu_a[hv_{avg}]}{\rho}\right)_{air}(hv)_{avg}\frac{1}{2}\int_h^\infty \frac{e^{-\mu_t[hv_{avg}]_{air}s}}{s}ds$$

(4)

8

Second Flight Contribution from Air Scatter

To calculate the contribution of once scattered gamma rays, we begin by imagining a differential volume located at some other location (X', Y') at a time of one hour and at a height h' (see Figure 3).
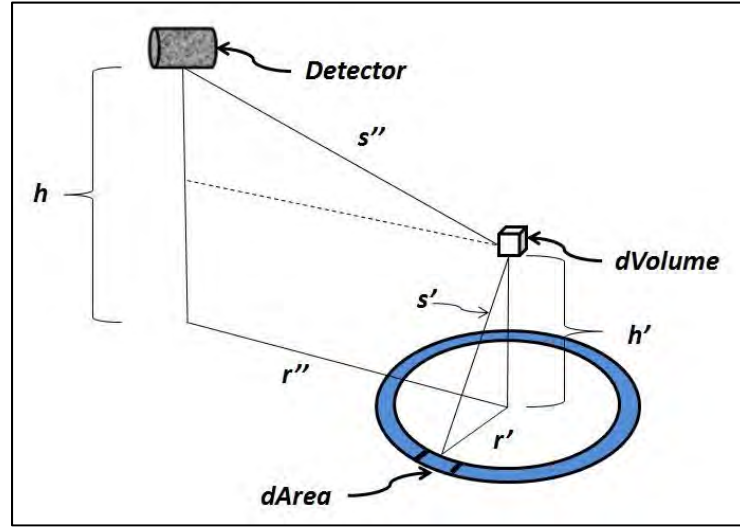
Figure 3. Representation of a differential volume as a scattering source.

This differential volume receives a direct flight contribution from the ground distributed fallout field. In this respect, the propagation of gamma rays to this differential volume is identical to the previous direct flight development with one exception: instead of being absorbed (as was the case for the detector), the gamma rays are scattered both coherently (Rayleigh) and incoherently (Compton) depending on cross sections. For now, we will assume the scatter is isotropic and incoherent. This concept is illustrated by the equation:

$$S_{air} = A_{gd} \ (\mu_s^o)_{air} \frac{1}{2} \int_{h'}^{\infty} \frac{e^{-(\mu_t^o)_{air} s'}}{s'} ds'$$

(7)

9

Note: Dependencies have been removed to simplify presentation of the equations

Where,

hv_o is the pre-scattered gamma ray energy in $[J]$;

μ_s^o is the scattering cross section at hv_o for air in $[m^{-1}]$;

μ_t^o is the attenuation cross section at hv_o for air in $[m^{-1}]$;

h' is the height of the differential volume in $[m]$;

s' is the slant range from the differential volume to a differential area on the ground in $[m]$ and

S is volumetric scattering source within the differential volume in $\left[\dfrac{Bq}{m^3}\right]$.

As viewed from the detector, this differential volume is identical to a volumetrically distributed source in air that is emitting at an activity S. Furthermore, this is only one of an infinite number of differential volumes in the space around the detector. As such, the contribution of *each* differential volume must be calculated in the form of a spatial integral:

$$\dot{D}_{SF}^{air} = \left(\frac{\mu_a'}{\rho}\right)_{air} (hv)' \int_0^\infty S_{air} \frac{e^{-(\mu_t')_{air} s''}}{4\pi r''^2} dVol$$

(8)

Where,

$\dot{D}_{SF}^{air}$ is the second flight contribution to dose rate in $\left[\dfrac{J}{kg - \sec}\right]$;

hv' is post-scatter gamma ray energy in $[J]$;

$\left(\dfrac{\mu'_a}{\rho} \right)_{air}$ is the total mass absorption coefficient of the detector for gamma rays at

energy hv' in $\left[\dfrac{m^2}{kg} \right]$; *Note: here an air equivalent point detector is assumed*

μ'_t is the attenuation cross section for air at hv' in $\left[m^{-1} \right]$;

r'' is the ground range from directly beneath the detector to directly beneath the

differential volume in $[m]$;

s'' is the slant range from the detector to the differential volume in $[m]$ and

$dVol$ is the differential volume defined as $2\pi r'' dr'' dh'$ in $\left[m^3 \right]$.

Similar to the FOM development, a change of variables must be accomplished to

homogenize the variable of integration. While temporarily holding h' constant:

$$s^2 = r^2 + \left| h - h' \right|^2 \text{ and } r'' dr'' = s'' ds''$$

Also associated with the change of variables is a respective change in limits of integration:

$$\text{When, } \begin{cases} r'' = 0 & s'' = \left| h - h' \right| \\ r'' = \infty & s'' = \infty \end{cases}$$

After executing the change of variables and once again allowing h' to vary, the result is:

$$\dot{D}_{SF}^{air} = \left(\dfrac{\mu'_a}{\rho} \right)_{air} (hv)' \dfrac{1}{2} \int_0^\infty S_{air} \int_{|h-h'|}^\infty \dfrac{e^{-(\mu'_t)_{air} s''}}{s''} ds'' dh'$$

(9)

The absolute value in the limit of integration necessitates further manipulation by

breaking up the integral into two parts based on the relationship between h and h'.

Physically, the integral is broken into the regions illustrated in Figure 4:

11
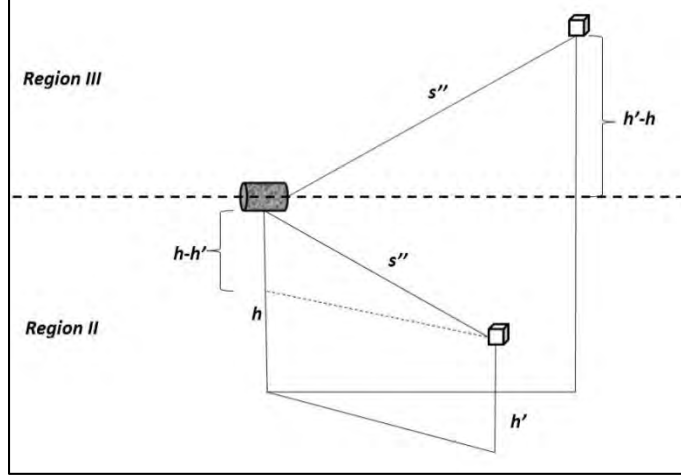
Figure 4. Regions II and III representing the space below and above the detector, respectively.

Substituting equation (7) for S and expanding the integral for *Region II* results in:

$$\dot{D}_{SF(II)}^{air} = C\left[\int_{0}^{h}\left(\int_{h'}^{\infty}\frac{e^{-(\mu_t^o)_{air}\,s'}}{s'}ds' + \int_{h-h'}^{\infty}\frac{e^{-(\mu_t')_{air}\,s''}}{s''}ds''\right)dh'\right]$$

(10)

The same is accomplished for *Region III* yielding:

$$\dot{D}_{SF(III)}^{air} = C\left[\int_{h}^{\infty}\left(\int_{h'}^{\infty}\frac{e^{-(\mu_t^o)_{air}\,s'}}{s'}ds' + \int_{h'-h}^{\infty}\frac{e^{-(\mu_t')_{air}\,s''}}{s''}ds''\right)dh'\right]$$

(11)

Where,

$$C = \frac{1}{4}(hv)'\left(\frac{\mu_a'}{\rho}\right)_{air} A_{gd}\ \mu_s^o$$

After the application of another change of variables for each region, the total contribution to dose rate from once scattered gamma rays in air is:

$$\boxed{\dot{D}_{SF}^{air} = C\left[\int_{0}^{h}E_1\left[\mu_t^o(h-u)\right]E_1\left[\mu_t'u\right]du + \int_{0}^{\infty}E_1\left[\mu_t^o(w+h)\right]E_1\left[\mu_t'w\right]dw\right]}$$

(12)

12

Second Flight Contribution from Ground Scatter

Given an isotropic emission of gamma rays from the ground distributed source, air scatter only addresses half of the emissions. The other half (which are ignored in the FOM) are gamma rays emitted directly into the ground which are absorbed, scattered into the ground, or scattered back into the air. Figure 5 illustrates the contribution of fallout to a differential volume in ground. Again, all scatters are still assumed to be isotropic at this point.
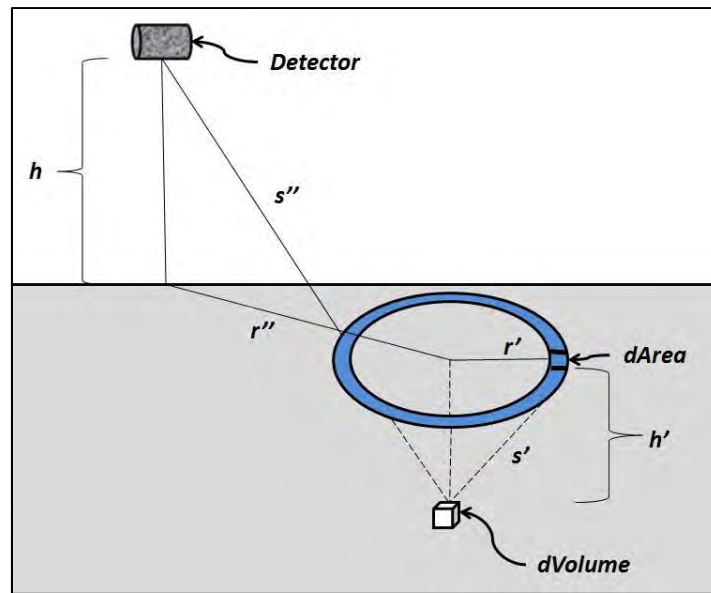
Figure 5. A differential volume representing a scattering source in the ground.

The contribution made to the detector from gamma rays once scattered in the ground begins similar to the air scatter development in equation (7) with the modeling of a source term describing the propagation of gamma rays to a differential volume:

$$S_{gd} = A_{gd} \ (\mu_s^o)_{gd} \ \frac{1}{2} \int_h^\infty \frac{e^{-(\mu_t^o)_{gd} s'}}{s'} ds'$$

(13)

13

The only differences from the previous source term development are the scattering and attenuation cross sections now reflect the change in medium from air to ground.

Also similar to the air scatter example is the development of the dose rate expression. Once scattered from the differential volume, the journey of gamma rays to the detector must be broken into two segments: one for ground, and one for air. This is illustrated in Figure 6:
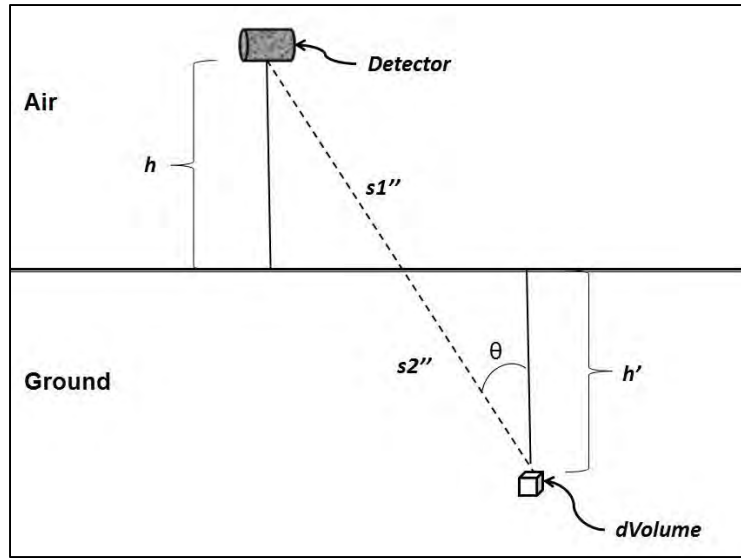
Figure 6. A gamma ray scattered within the ground must travel through both ground and air as it proceeds to the detector.

$$\dot{D}_{SF}^{gd} = \left(\frac{\mu_a'}{\rho}\right)_{air} (hv)' \frac{1}{2} \int_{h+h'}^{\infty} S_{gd} \frac{e^{-(\mu_t')_{gd} \, s2'' - (\mu_t')_{air} \, s1''}}{s''} ds''$$

(14)

Where,

$s1''$ is the slant range distance covered in the air in $[m]$ and

$s2''$ is the slant range distance covered in the ground in $[m]$.

After applying some trigonometry and a change of variables, the end result is:

14

$$\dot{D}_{SF}^{gd} = C \int_{h}^{\infty} E_1 \left[\left(\mu_t^o \right)_{gd} (u-h) \right] E_1 \left[\left(\mu_t' \right)_{gd} (u-h) + \left(\mu_t' \right)_{air} h \right] du$$

(15)

Finding Post-Scatter Energy

Before a build up factor (BUF) is calculated, a few hurdles remain in obtaining a value for hv' contained in the constant term (C) of equations (12) and (16). Using the three basic conservation equations, *The Atomic Nucleus* gives us the following relationship for Compton scatter (Evans, 1955:675):

$$\frac{hv'}{hv_0} = \frac{1}{1+\alpha(1-\cos\vartheta)}$$

(16)

Where,

hv' is the post-scatter energy in $[MeV]$;

hv_0 is the incident energy in $[MeV]$;

α is the value $\dfrac{hv_0}{m_0 c^2}$ and

ϑ is the photon angle of deflection.

This relationship illustrates the direct correlation between angle of deflection and post-scatter energy. Accounting for all possible angles and post-scatter energies for all incident energies is extremely challenging, thus a simplifying approximation is made in using an *average* angle of deflection to determine an *average* post-scatter energy. This is accomplished using a derivation of the Klein-Nishina formula to find the angular distribution of Compton scattered photons (Evans, 1955:690):

$$\frac{d(_e\sigma)}{d\vartheta} = \frac{d(_e\sigma)}{d\Omega} 2\pi \sin\vartheta$$

(17)

15

Using an expanded version of equation (17), a plot is generated for the 0.70MeV case (shown in Figure 7):
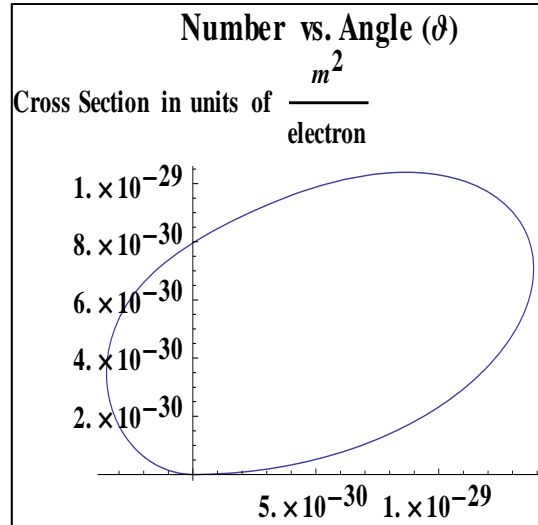
Figure 7. Plot representing the number of scattered photons per unit angle

By integrating equation (17) from 0 to π, the entire area of the lobe displayed in Figure 7 is calculated. Using this value as a normalization factor, a weighted average of the number of photons per angle is taken to obtain an average angle of scatter. This average angle is used in equation (16) to obtain an average energy ratio, which is then multiplied by the incident energy to get an average post-scatter energy.

Ground Non-isotropic Adjustment Term

Even though Figure 7 is evidence of the contrary, up to this point it is assumed that all scatters are isotropic. As shown in Figure 8, this assumption clearly breaks down as energy increases and gamma rays are preferentially scattered in the forward direction.
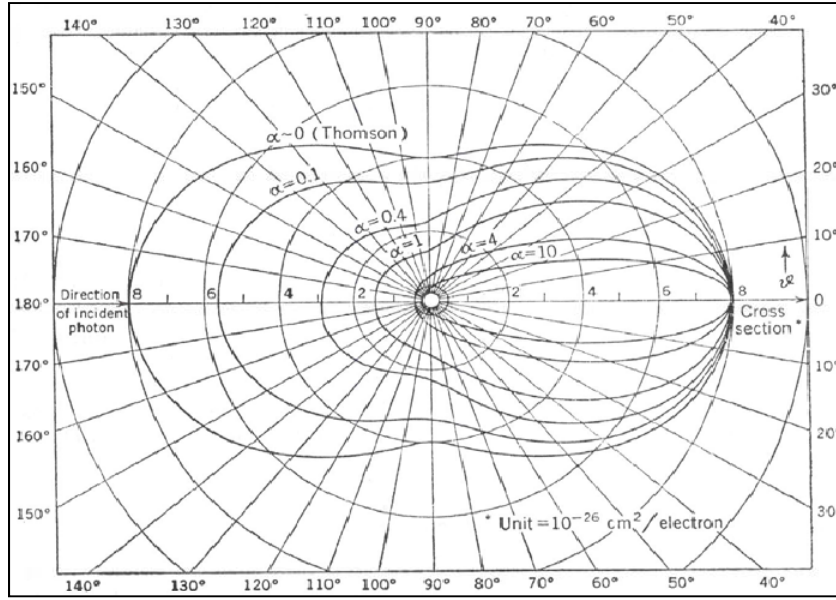
Figure 8. Klein-Nishina plot from *The Atomic Nucleus* (Evans, 1955:683)

Accounting for all possible scattering angles using an integral method is challenging; however, a rough approximation can be made in the case of ground scattered gamma rays to further refine the model. Given a fallout field distributed over a smooth surface, the range of possible scattering angles a gamma ray could achieve in ground *near the detector* in order to scatter back into the air is 90°-270°. Therefore at any given energy, the ratio of the backscatter region area (90°-270°) to the area of the entire scattering range (0°-360°) gives a rough estimate of the fractional portion of ground scatter that returns to the air.

The obvious flaw in this adjustment term is that gamma ray emissions from large horizontal distances may graze the ground, and forward scatter towards the detector. This is why the stipulation "*near the detector*" is necessary when describing the development of this term. This value is designated as the Ground Non-isotropic Adjustment Term (GNAT).

The Build-up Factor (BUF)

The total dose rate experienced from once scattered gamma rays at the detector is:

$$\dot{D}_{SF}^{total} = \dot{D}_{SF}^{air} + \dot{D}_{SF}^{gd}$$

From this value a build up factor (BUF) is established by:

$$BUF = 1 + \frac{\dot{D}_{SF}^{air} + \dot{D}_{SF}^{gd}}{\dot{D}_{DF}}$$

(18)

Additional terms may be incorporated with the BUF, as is the case for the limited second scatter approximation.

Limited Second Scatter Approximation

Using the previous figures as a reference, another approximation can be made to further refine the BUF. As seen from the detector, any gamma ray that scatters in ground and returns to the air is identical to a ground distributed source emitting at the average post-scatter energy. This secondary source can then scatter in air before making an additional contribution to the detector.

This temporarily assumes that scatter in ground is completely isotropic – but for purposes of this additional refinement to the BUF, the approximation is sufficient. Mathematical development of the contributions of this additional term is identical to that of the second flight air contribution derivation from a previous section (see page 9).

III. Scattering Contributions to the Build Up Factor

The Modeling Environment

To obtain the results discussed in this section, various assumptions about air and ground composition are made. The reader is cautioned that every number reported in this section is not absolute, and must be associated inseparably with these assumptions and approximations. In other words, consider all values to have qualitative error bounds associated with the various assumptions used in this model.

In all models, ground is assumed to be homogeneous in both composition and density. As ground composition varies significantly, a simplification is made by assuming a chemical composition of 100% SiO_2. Also varying with composition, location, compaction, and several other factors is soil density. Density values range anywhere from 1000-2000 kg/m^3 for sandy soils, so a simplified value of 1922 kg/m^3 is arbitrarily assumed. Finally, the ground is assumed to be a perfectly smooth and level plane (assumption #5 of the FOM).

Applied to all models, air is assumed to contain 78% N_2 / 21% O_2 / 1% Ar. Following the International Standard Atmosphere, a temperature and density of 15°C and 1.23 kg/m^3 for sea level air are observed. These parameters are taken as universal and homogenous at all locations and altitudes.

Fallout distribution is assumed to be homogenous and unfractionated in all cases. As stated in the FOM, the activity density directly under the detector is assumed to be uniform at all locations. The variation of activity density over the distribution of fallout is analyzed in Chapter V.

For cases involving a single average gamma ray energy, the source is assumed to emit at the specified average energy in an isotropic fashion. In evaluation of the entire fallout

energy spectrum, activity weighted values are used to describe the fractional energy

contribution of each individual energy group. These fractional contributions are assumed to

be constant at all locations.

As previously stated, all scattering events are assumed to be isotropic unless otherwise

noted. This assumption is obviously incorrect as shown in the Klein-Nishina plots (Figure 8);

however, it is assumed that the overestimation of scattering contributions for trajectories

pointed away from the detector will partially balance with the underestimation of scattering

events that occur for trajectories pointed at the detector. The quality of this assumption is not

addressed and it is listed as a simplifying assumption.

Fundamental to modeling all photon interactions with matter are cross sections. All

cross section values were obtained from the National Institute of Standards and Technology

(NIST) XCOM Photon Database. For energies not listed on the table, a simple linear

interpolation scheme (on a log-log plot) is used.

Finally, sample calculations for each of the numerical values reported in this chapter

may be found in *Appendix A* referenced by superscripts following each reported value in this

chapter.

The Case for a Single Incident Average Energy

As proposed in *The Effects of Nuclear Weapons* (Glasstone, 1977:454), the average energy

of all gamma rays at a time of one hour after detonation is 0.70MeV. Using the techniques

previously discussed in Chapter II, 0.70MeV gamma rays Compton scatter down to an average

energy of approximately 0.38MeV[5]. At this post-scatter energy, isotropic scattered gamma rays

---

[5] See Appendix A (1)

in air contribute 7.5%[6] of the dose rate as seen by the detector – with 83%[7] of the air scattering contribution coming from Region III (the region above the detector). In addition, isotropic gamma ray scatter from the ground contributes 6.1%[8] of the total dose rate.

After making further adjustments for non-isotropic ground scatter using the Ground Non-isotropic Adjustment Term (GNAT) and adding the contributions from the limited second scatter approximation, the final BUF value for single average incident energy of 0.70MeV is calculated to be 1.1.[9] These values result in a source normalization constant of[10]:

$$\text{SNC for 0.70MeV and BUF of 1.1} = 7.5 \times 10^{-16} \left[\frac{J - m^2}{kg - \sec - Bq} \right]$$

This new SNC replaces the constant previously mentioned in equation (6). These results indicate that scattering contributes at least 10% to the SNC.

The impact of the BUF is not constrained to a single energy, however. As such, the BUF value associated with a single average gamma ray energy of 0.70MeV must be contrasted with BUF values for the actual distribution of fallout energy to further gauge its quality as an assumption.

The Case for Multiple Incident Energies

As illustrated in Figure 9, the previously discussed average gamma ray energy 0.70MeV falls within the Compton scattering/absorption region for air. In the energy range of 0.30MeV – 1.0MeV, the lines for total absorption, total attenuation, and Compton scattering are fairly

---

[6] See Appendix A (2)

[7] See Appendix A (3)

[8] See Appendix A (2)

[9] See Appendix A (4)

[10] This value is computed by multiplying the previous SNC of 6.8x10⁻¹⁶ by the BUF of 1.1

constant and remain in the same order in terms of the mechanisms of matter interaction. However, the region to the far left (roughly 0.02MeV – 0.10MeV) relative cross sections have steeper slopes. The question then becomes, what impact might this have on the BUF? And, will this impact be significant enough to further change the source normalization constant?
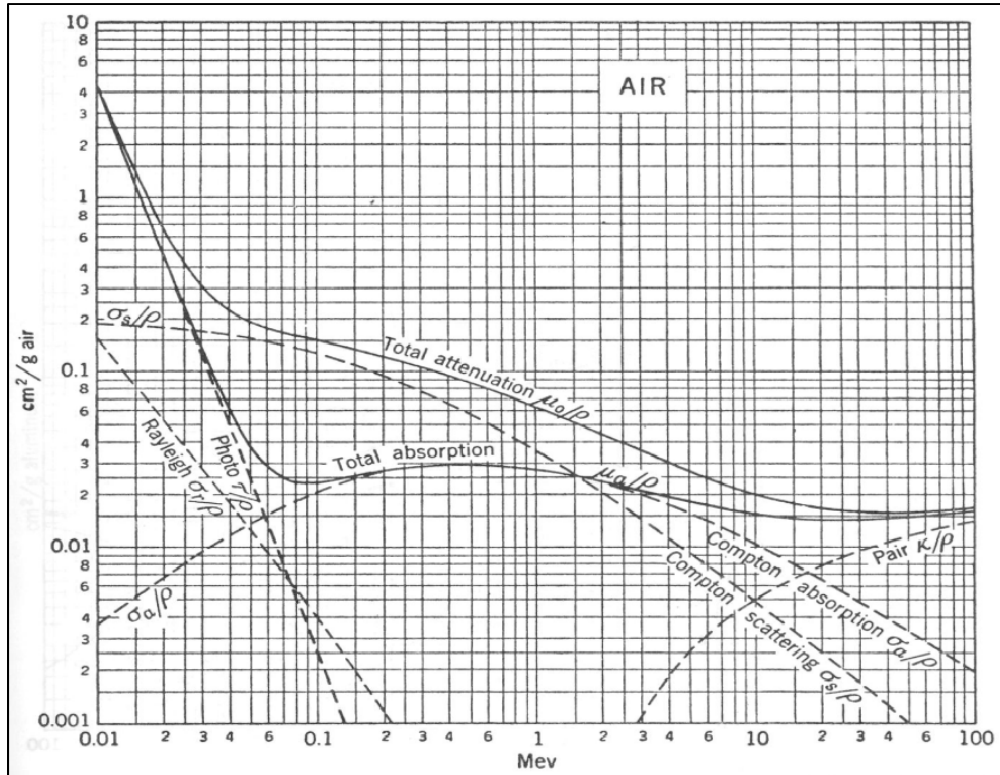
Figure 9. Mass coefficients for air from *The Atomic Nucleus* (Evans, 1955:713).

Utilizing the identical model and method used for the single average incident energy case, multiple incident energy groups were analyzed to determine a BUF across the spectrum of interest. The specific breakdown of these energy groups and the rationale for the energy range depicted are addressed in Chapter IV. These results are displayed in Figure 10:

22
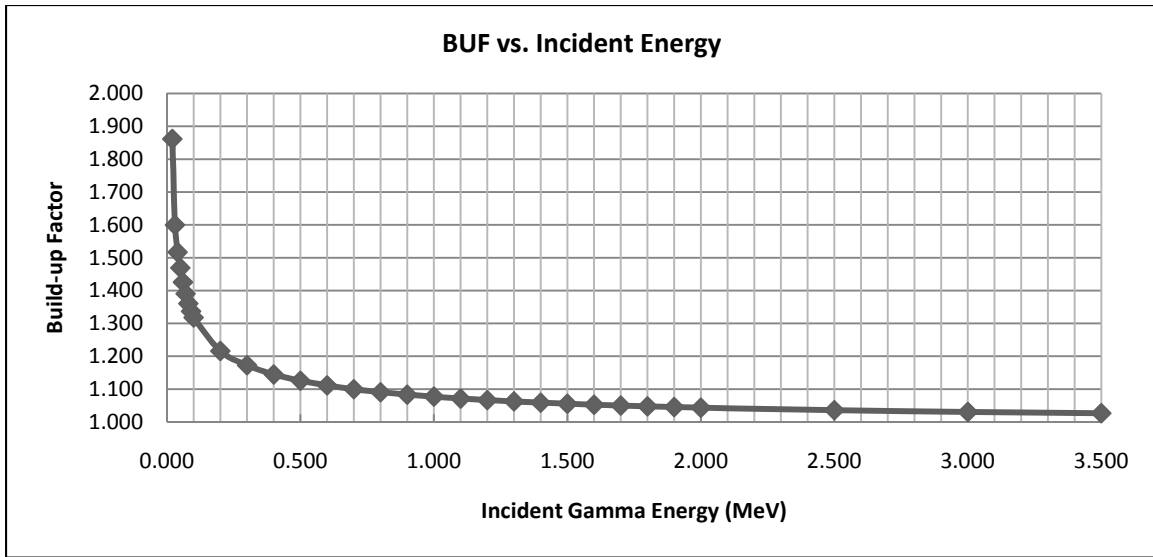
Figure 10. The BUF as a function of incident gamma energies[11]

As shown in Figure 10, the BUF rises to nearly 1.9, rapidly declines, and then asymptotically approaches a value close to 1.0. This relationship is explained by understanding the inherent limitations to the BUF value and a brief analysis of cross sections.

The first observation is the apparent asymptotic approach to a BUF of 1.0 as energy increases. This can be attributed to a combination of cross section behavior and the energy lost due to a scattering event at high energies. Shown in Figure 11, as energy increases the amount of energy lost due to a scattering event also increases.

---

[11] This chart is the result of the BUF development from the previous section applied to multiple energies.
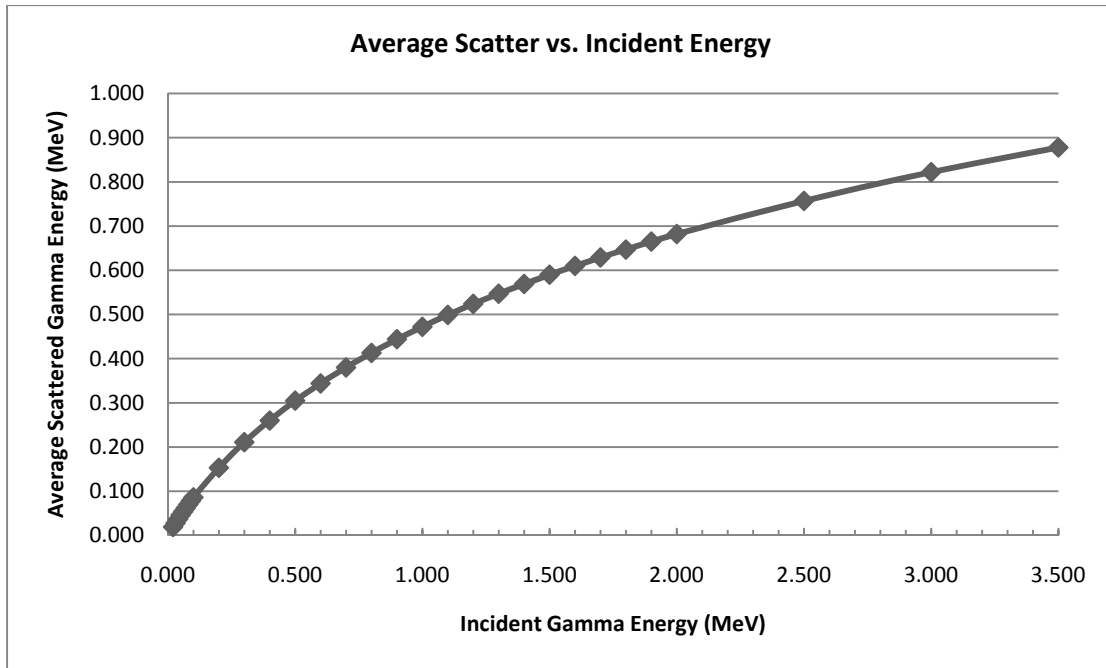
Figure 11. Average scattered energy as a function of incident energy[12]

The larger the amount of energy loss, the greater the shift to the left on Figure 9 for post-scatter energy – which means a greater change in relative cross section values from pre to post collision. In the region of interest for nuclear fallout (0.0MeV – 3.5MeV), a shift to the left universally equates to an *increase* in total attenuation cross section and a *decrease* in mean free path. This creates a situation where high energy gamma rays have the energy to travel far away from the detector before interacting with matter; however, once they interact and lose a significant fraction of their energy, their chances of making the same trip *back* to the detector without attenuating are severely reduced. As such, the BUF is expected to asymptotically approach a value close to 1.0 as energy increases.

---

[12] This chart is an application of Appendix A (1) across multiple energies.

Figure 10 also exhibits a peak in BUF value associated with lower energies. Again, this feature is explained by analyzing the cross sections featured in Figure 9. In this case, the energy lost in low energy collisions is less than 1%. Nonetheless, even the smallest decrease in energy results in a relatively large increase in absorption cross section, yet only small relative change in scattering cross section. In this scenario, low energy gamma rays will tend to scatter (losing very little energy in the process) until absorbed by the detector.

The BUF value for the range below 0.02MeV is associated with the physical geometry of the problem and is predicted to eventually decline to a value of 1.0. This concept is best described using Figure 12:
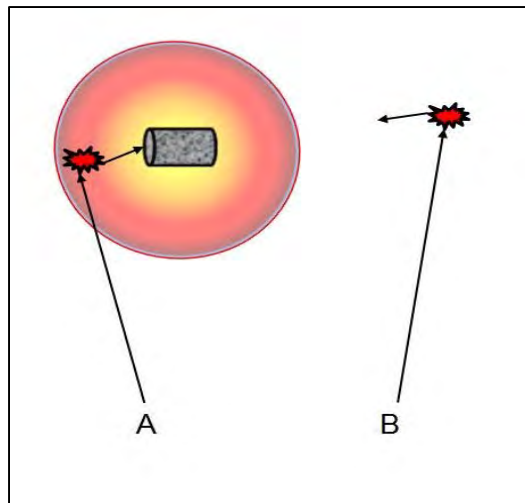
Figure 12. Geometric limitations of low energy scatters

Consider two identical gamma rays (A and B) emitted from the ground. If the problem is constrained such that a gamma ray *must* scatter once before reaching the detector, there is a limited volume of interaction (shown above as the sphere surrounding the detector) in which a gamma ray can scatter and still have a significant probability of arriving at the

detector. In Case B, the gamma ray scatters outside this limited volume and does not possess the energy to have a significant probability of reaching the detector. As energy decreases, the proximity of the scattering event to the detector must also decrease if the gamma ray is to reach the detector. Likewise as energy increases, the proximity of the scattering event may occur at larger distances. The concept of this limited volume of interaction in the form of a sphere is also vital in describing the relative contributions of air scatter and ground scatter to the detector (Figure 13).
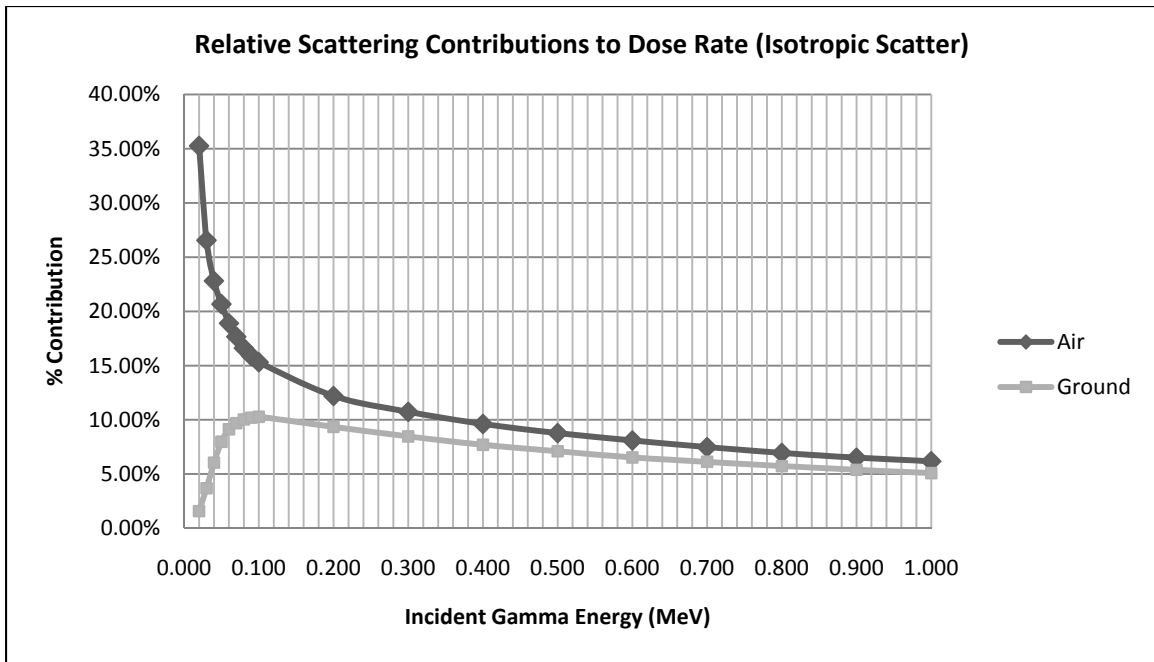
Figure 13. Relative contributions of scattered energy from air and ground[13]

As shown in Figure 13, air is the dominant source in scattering contributions to the detector. Conceptually, this is understood by comparing the two mediums. In air, attenuation

---

[13] This chart is an extension of the values calculated in Appendix A (4) across multiple energies.

cross sections are fairly low. This allows for mean free paths of 18 meters[14] for a 0.02MeV

gamma ray and 110 meters for a 0.70MeV gamma ray. Mean free paths on the order of 100

meters mean gamma rays have the ability to traverse much larger distances and still reach the

detector. Conversely, ground attenuation cross sections allow for mean free paths of

2.1×10^{-3} meters for 0.02MeV gamma rays and 7.8×10^{-2} meters for 0.70MeV gamma rays.

These values suggest that unless the scattering event occurs extremely close to the surface –

the gamma ray will likely never make it out of the ground.

A less obvious observation is the energy at which relative contributions from these two

mediums peak are different. This is explained by referencing Figures 11 and 12.   The air

contribution peak occurs at roughly 0.02MeV. At this energy, the limited volume of

interaction described in Figure 12 is in optimum balance. An increase in energy from this point

of balance would increase the limited volume of interaction, but that increase in volume would

actually result in a *decrease* in first scatter contributions to the detector. This decrease is because

of spherical divergence and the previously described case of a gamma ray having enough

energy to travel a large distance before scattering, but not having enough energy to return.

Likewise, a decrease in energy from the point of balance would result in a decrease in the

limited volume of interaction. This smaller volume equates to a smaller quantity of gamma

rays being able to scatter and still make it to the detector. In essence, the air contribution peak

in Figure 13 is a result of the Goldilocks adage applied to the volume of interaction – not too

big, not too small, but just right.

As it turns out, this ideal limited volume of interaction for air is far from ideal for

ground. Although ground contributions are on the rise at 0.02MeV, they are not at a peak.

_____

[14] Appendix A (5)

This is because the aforementioned volume of interaction only barely intersects the ground, meaning the volume of air available for interaction dwarfs the volume of ground available (see Figure 14).
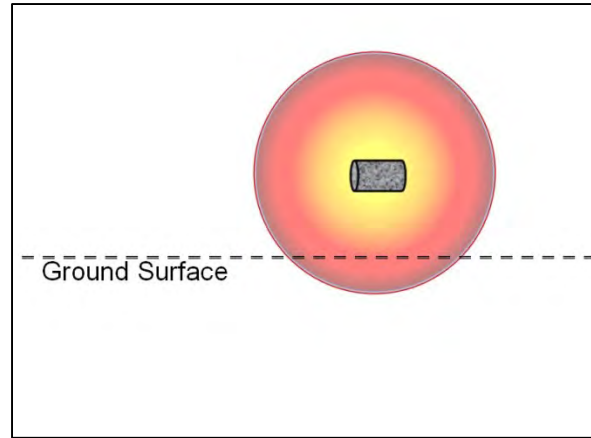
Figure 14. Limited volume ground interaction.

Because of the minor amount of ground contained within the limited volume at 0.02MeV, it is understandable that scattering contributions from the surface will be relatively minor – especially considering ground interactions are more dependent upon surface area than volume as described before with mean free path comparisons. Furthermore, any ground interaction will also need to traverse a volume of air before reaching the detector. After energy increases to approximately 0.10MeV, the volume of limited interaction grows into the previously mentioned balanced condition for the same reasons – only this time conditions are optimized for ground scatter contributions.

Another observation is that ground scatter contributions never exceed the contributions of air scatter, but instead approach a state of almost identical contribution at higher energies. Again, using the concept illustrated in Figure 14 this makes sense. The volume of air within the limited volume of interaction will *always* exceed the corresponding

volume of ground because the reference volume is centered on the detector. This disparity in volume that dominates low energies becomes less apparent as the limited volume of interaction grows with increasing energy. As the disparity in volume becomes less pronounced, the difference in relative air and ground scatter contribution also becomes less pronounced.

Finally, a caution must be observed. Although the mechanics of these interactions occur as previously described, definitively associating these peaks with a specific gamma ray energy is somewhat misleading. The fact that the BUF peak occurs at roughly 0.02MeV is merely a product of how the information is presented (in terms of incident energy) and how many scatters are allowed (one). If the BUF is plotted as a function of incident energy while *only considering two scatters* – the relative BUF peak would appear at slightly higher incident energy. The effect of considering multiple scatters is predicted to broaden the peak observed in Figure 10, effectively expanding higher BUF values across a larger spectrum of energy. This fact further emphasizes the need to expand research of this problem into multiple scatters.

Regardless of how many scatters are considered, Figure 10 demonstrates a definitive energy dependence of the BUF term. Because of this dependence, the BUF value of 1.1 for an average energy of 0.70MeV may not be representative of the actual fallout energy distribution. Depending on which energies dominate the spectrum, the higher BUF values associated with lower energies may further influence the source normalization constant. This issue is examined in the next chapter.

IV. Challenging the 0.7MeV Average Energy of Fallout

As previously discussed, assumption #2 in the development of the FOM reduces the

full spectrum of energy emitted from the fallout field to a single average gamma ray energy of

0.70MeV. In Chapter III, results from Figure 10 show a definitive energy dependence of the

BUF value. Depending on the energy distribution of fallout, the higher BUF values associated

with other energies could impact the calculated value for a source normalization constant at

one hour post detonation. As such, the objective of this chapter is twofold: First, to verify the

accuracy of using 0.70MeV as the average photon energy emitted from a fallout field at a time

of one hour. Once the average is verified, the second objective is to determine if using average

photon energy is a reasonable approximation in calculating a BUF and the resulting source

normalization constant.

Using the ORIGEN Fallout Analysis Tool provided by Oak Ridge National

Laboratory, fallout energy distributions for two different fission types were analyzed. Fissile

material compositions are taken as 90%/10% Uranium-235/Uranium-238 respectively, and

100% Plutonium-239. Both fuels are assigned a yield of 1 Kiloton and contain 1.0kg of

material[15]. The specific procedure and model values used in these simulations are addressed in

Appendix B while actual code output may be found in *Appendix C.*

---

[15] 1.0kg of fissile material cannot produce a 1kt yield; however, proportions of the isotope inventory are unaffected by fuel mass. As such, assuming a 1.0kg mass does not affect the values obtained in this chapter.

Average Energy and Total Photon Activity for 100% Pu-239 Fission

The energy spectrum from 0.0MeV to 5.0MeV is broken up into 50 energy groups of equal energy (Figure 15). This range accounts for ~100% of all energy of the distribution at one hour[16]. From there, an activity weighted average is used to calculate the average photon energy and total activity within the ORIGEN Fallout Analysis Tool.
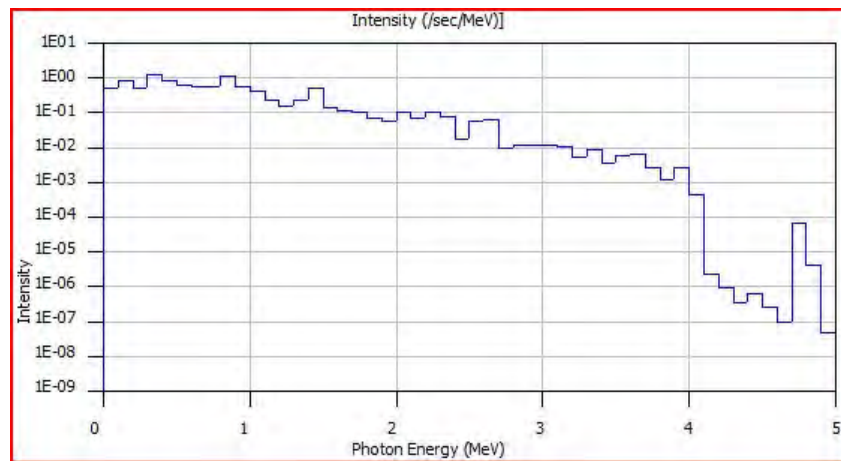
Figure 15. The energy spectrum of fallout from 100% Pu-239 fission at one hour.

The average photon energy for Pu-239 fission is found to be 0.79MeV[17], while the total activity is shown to be 595 Photon Megacuries[18]. These results are shown in Figure 16.

---

[16] See the last lines of Figure 16 to obtain the "not counted" portion of energy

[17] See *Appendix B* for model parameters

[18] This value is for gamma rays and x-rays

```
--------------------------------------------------------------
Photon Source Definition - generated from ORIGEN F71 file
  Filename: today.f71
    case 106.  3.600E03 seconds   0.000E00
  total strength:  2.2051E19 gammas/second
  average energy:   0.7865806796307987
  discrete lines:  0.0000E00 gammas/second
                   0.00% of energy
  average line energy:   0.0
  multigroup bins: 2.2051E19 gammas/second
                   100.00% of energy
  average group energy:   0.7865806796307987
  not counted:      1.4098E11 gammas/second
                   0.00% of the original energy
--------------------------------------------------------------
```

Figure 16. Results from ORIGEN Fallout Analysis Tool for average energy and total photon activity of fallout from Pu-239 fission at one hour.

Since these results deviate from the widely accepted values of 0.70MeV and 530 Gamma Megacuries[19] in *The Effects of Nuclear Weapons* (Glasstone, 1977:454), another composition is analyzed to ensure that fuel composition is not a dominating factor in the values obtained for average energy and total photon activity.

Average Energy and Total Activity for 90/10 U-235/U-238 Fission

The energy spectrum from 0.0MeV to 3.5MeV is broken up into 35 energy groups of equal energy. This range accounts for 99.6% of all energy of the distribution at one hour[20]. From there, an activity weighted average is used to calculate the average gamma ray energy and total activity within the ORIGEN Fallout Analysis Tool. The average gamma ray energy is found to be 0.81MeV[21]. This is in contrast with the 0.70MeV average listed in *ENW*.

---

[19] Although this value includes only gamma rays, the lack of X-ray inclusion does not account for the 65 Megacurie difference.

[20] See the last lines of Figure 17 to obtain the "not counted" portion of energy

[21] See *Appendix B* for model parameters

Likewise, total gamma ray activity is shown to be 583 Gamma Megacuries – compared to the

530 Gamma Megacuries listed in *ENW*. These results are shown in Figure 17.

Figure 17. ORIGEN Fallout Analysis Tool output for average energy and total activity at 1 hour for a 90/10 U-235/U-238 fission.

To convert from "total strength" to Gamma Megacuries, the following relationship is used:

$$\text{Total Activity} = \frac{\text{Total Strength}\left\{\dfrac{\text{gamma rays}}{\text{sec}}\right\}}{3.7\times10^{16}\left\{\dfrac{\text{gamma rays}}{\text{sec-megacuries}}\right\}} \tag{19}$$

The differences in these values from those used within *ENW* are of unknown origin,

but most likely can be attributed to the use of modern data sources (such as improved cross

sections and fission yield values) contained within the ORIGEN Fallout Analysis Tool.

Inclusion of X-rays into the Model

In regards to the source normalization constant (SNC), gamma rays are not the only source of photons contributing to dose rate. These X-rays originate from capture and de-excitation of electrons by fission products. Another potential excitation mechanism is ejection of an inner shell electron. In this case, the remaining electrons shift to fill the inner shell vacancy and emit X-rays in the process. Regardless of the excitation mechanism, excited electrons shifting to a ground state in elements containing more than six protons cause the emission of X-rays.

X-rays also contribute to the dose rate seen by the detector. As such, an additional simulation including X-rays is also analyzed. In Figure 18, the inclusion of X-rays results in a 0.01MeV increase in average photon energy. After using equation (20), total activity shows an increase to 605 Photon Megacuries.


```
------------------------------------------------------------
Photon Source Definition - generated from ORIGEN F71 file
   Filename: today.f71
      case 106.   3.600E03 seconds    0.000E00
   total strength:  2.2393E19 gammas/second
   average energy:   0.8220924456853023
   discrete lines:  0.0000E00 gammas/second
                    0.00% of energy
   average line energy:    0.0
   multigroup bins: 2.2393E19 gammas/second
                    100.00% of energy
   average group energy:    0.8220924456853023
   not counted:     5.5186E16 gammas/second
                    1.10% of the original energy
------------------------------------------------------------
```

Figure 18. ORIGEN Fallout Analysis Tool output for average energy and total activity at 1 hour for a 90/10 U-235/U-238 fission including X-rays.

Because the SNC is independent of activity density, the change in average energy and group weighting are the only possible impacts of X-ray inclusion. Nonetheless, all weighting values used in the calculation of SNCs from this point forward combine both gamma ray and X-ray contributions.

SNC for 90/10 U-235 Fission Using Multi-Group Approach

In order to gauge the effect of the energy dependent BUF value on the SNC, the energy spectrum from 0.0MeV to 3.5MeV is broken up into 35 energy groups (see Figure 19). In order to gain increased resolution over the region where the BUF varies significantly, the range of 0.0MeV to 0.10MeV is further divided into 10 subgroups.
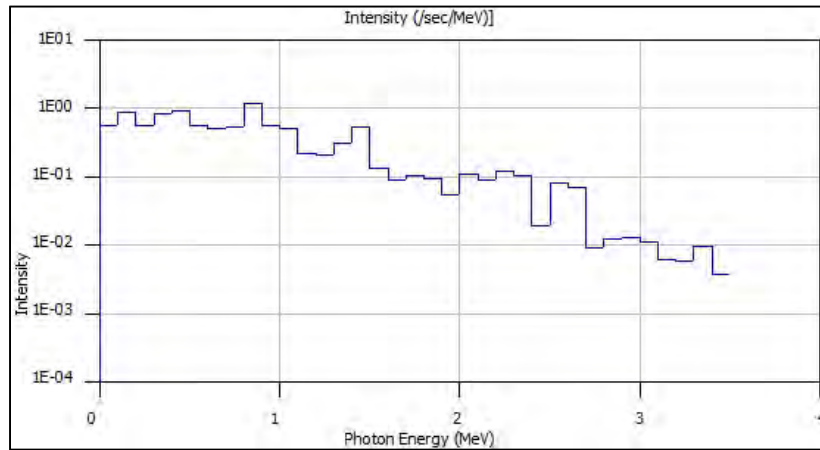
Figure 19. ORIGEN Fallout Analysis Tool Photon Source output showing the distribution of energy and intensity.

Using the process described in Chapters II and III, the BUF and SNC values are calculated for each individual energy group (see Figure 20)[22].
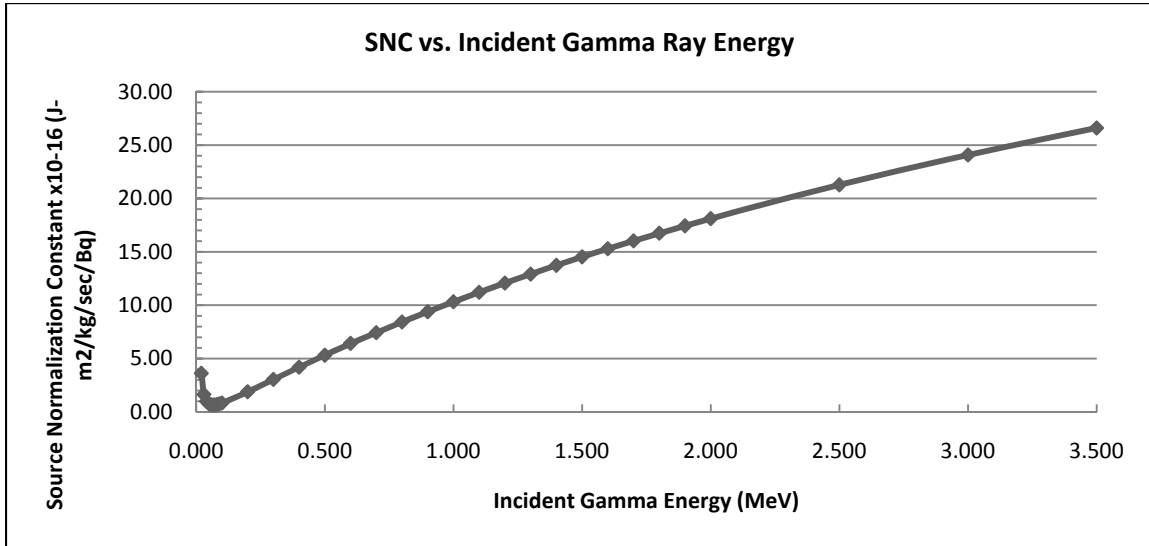
Figure 20. Source Normalization Constant as a function of incident gamma ray energy.

Once calculated, these values are paired with weight values generated by the ORIGEN Fallout Analysis Tool and combined to generate a total SNC. The result of using a multi-group approach to calculate a SNC for the spectrum of 0.0MeV - 3.5MeVat a time of one hour post detonation is[23]:

$$\text{Multi-Group } SNC = 8.6 \times 10^{-16} \left[\frac{J - m^2}{kg - \sec - Bq} \right]$$

---

[22] BUF values for each energy group are shown in Figure 10

[23] *Appendix D* contains all tabled weight values used to calculate this value

This value is 15% greater than the SNC value determined in Chapter III. The source of this difference is discussed in "Addressing the Difference in Source Normalization Constant" section.

SNC for 90/10 U-235 Fission Using Average Energy and BUF Values

After determining the total SNC based on a multi-group approach to the energy spectrum, another SNC is calculated using the average energy of 0.81MeV and an *average* BUF value for the energy distribution. The average BUF value is calculated using the weight values generated by the ORIGEN Fallout Analysis Tool combined with a specific BUF value calculated for each individual energy group. This yields an average BUF value of 1.1.[24] The SNC calculated using this method is[25]:

$$\text{Average BUF SNC at 0.81MeV} = 8.6 \times 10^{-16} \left[\frac{J - m^2}{kg - \sec - Bq} \right]$$

This result is identical to that of the multi-group approach in the previous section. This confirms that the use of a single average photon energy and *average* BUF value is an accurate approximation in calculating the SNC.

Addressing the Difference in Source Normalization Constant

Recall the SNC calculated in Chapter III uses an average gamma ray energy of 0.70MeV. This is in immediate disagreement with the ORIGEN Fallout Analysis Tool

---

[24] *Appendix D* contains all tabled weight values used to calculate this value

[25] This calculation shown in *Appendix A (6)*

estimate of 0.81MeV. If the method of calculating the SNC contained in this chapter is accurate, the SNC calculated using an average gamma ray energy of 0.70MeV should match the value calculated in Chapter III.   Therefore, the entire process from the previous section is repeated using an average energy of 0.70MeV and average BUF of 1.1. Using these parameters, the SNC is determined to be[26]:

$$\text{Average BUF SNC at } 0.70\text{MeV} = 7.5 \times 10^{-16} \left[\frac{J-m^2}{kg-\text{sec}-Bq} \right]$$

This value represents a match with the SNC value obtained in Chapter III and demonstrates that the difference in SNC values are due to the use of 0.81MeV as the average photon energy.

Fallout Distribution Analysis SNC Results

From these results, two observations are made: First, the average energy of a fallout field is 0.81MeV instead of 0.70MeV as calculated by the ORIGEN Fallout Analysis Tool. Second, the assumption of a single average gamma ray energy with an average BUF is shown to be a reasonable approximation. Although the BUF changes significantly in the energy range 0.0MeV to 0.50MeV, the relative contributions of those energy groups are minor in comparison to the spectrum as a whole. However, these results are still limited by the assumptions made in the development of this model (discussed in Chapters II and III). With

---

[26] Since the BUF value of 1.1 is confirmed in this chapter, this calculation contains identical values to those used in Chapter III (page 21)

these modifications originating from the fallout distribution analysis in this chapter, the SNC is

further refined to a value of:

$$\text{Updated SNC} = 8.6 \times 10^{-16} \left[\frac{J - m^2}{kg - \sec - Bq} \right]$$

$$\text{Updated SNC} = 2900 \left[\frac{R - mi^2}{hr - KT} \right]$$

Note: The calculated activity per kiloton of fission yield (583 Gamma Megacuries for 90/10 U-235/U-238, for example) does not impact the value of SNC in mks units; however, it does impact the conversion of the SNC to the traditional units of $\left[\dfrac{R - mi^2}{hr - KT} \right]$, *because the number of (Bq) in a (KT) of fission yield changes depending on the fuel used. This fact strongly reinforces the use of mks units as the standard in discussing SNCs.*

V. Varying Activity Density

In the previous chapters, assumptions regarding the source normalization constant (SNC) were analyzed. As shown in equation (6), activity density is also an influential term in determining dose rate. Stated in assumption #4, the first order model (FOM) assumes the activity density directly beneath the detector is uniform out to infinity. Removing the spatial dependence of activity density allowed it to be removed from the integral as a constant:

$$\dot{D}[X,Y,1] = A[X,Y,1]\left(\frac{\mu_a[hv_{avg}]}{\rho}\right)_{air}(hv)_{avg}\frac{1}{2}\int_h^\infty \frac{e^{-\mu_t[hv_{avg}]_{air}\,s}}{s}ds \tag{3}$$

In reality, there *is* a spatial dependence on activity density; therefore, this assumption must be analyzed to gauge its impact on calculating dose rate.

Activity Deposition on the Ground

In the *Introduction to the Physics of Nuclear Weapons Effects,* Bridgman discusses the formulation of a model for activity distribution on the ground incorporating both vertical settling and horizontal wind transport (Bridgman, 2001:411). In this equation the lateral spatial distribution (modified to use variables consistent with this thesis) is[27]:

$$A[r,t] = A[t]\left\{\frac{1}{\sqrt{2\pi}\sigma_r}e^{-\frac{1}{2}\left(\frac{r}{\sigma_r}\right)^2}\right\} \tag{20}$$

Where,

$A[r,t]$ represents the activity density at a position r [m] and at time t [sec] ;

$A[t]$ is the activity density at time t, and

σ_r is the standard deviation of the fallout distribution in [m].

---

[27] Bridgman equation (12-24)

This expression makes several assumptions. First, it assumes a normalized Gaussian distribution in horizontal directions. Although toroidal motion during cloud rise creates a ring shaped distribution (Jodoin, 1994:91-93), ground fallout patterns suggest a transition to a Gaussian distribution occurs sometime during cloud fall (Bridgman, 2001:407). For purposes of this discussion, we also assume no wind. The result of this assumption would be a circular fallout pattern centered on ground zero. Although this assumption is unrealistic, it actually represents the worst case scenario in terms of activity density varying with respect to distance from the detector. In other words, a "smeared" Gaussian distribution only in the horizontal axes presents a larger standard deviation. Finally, we assume the standard deviation of fallout is symmetric – further leveraging the no wind assumption.

The distribution represented in equation (20) is inserted into the integral in equation (3). The result is equation (21), where the normalization factor $\frac{1}{\sqrt{2\pi}\sigma_r}$ is removed to create a correction factor that maintains a value between 0 and 1. This result is shown in Figure 21.
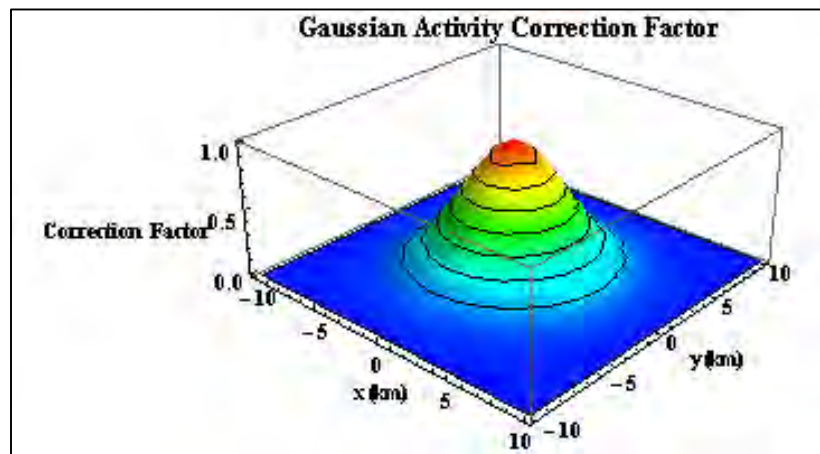
Figure 21. The Gaussian Activity Correction Factor

41

Thus we have defined a correction factor:

$$\text{Correction Factor} = \frac{\displaystyle\int_{h}^{\infty} \frac{e^{-\left(\mu_t [hv_{avg}]_{air} s\right)} e^{-\frac{1}{2}\left(\frac{s^2 - h^2}{\sigma_r^2}\right)}}{s} ds}{\displaystyle\int_{h}^{\infty} \frac{e^{-\left(\mu_t [hv_{avg}]_{air} s\right)}}{s} ds}$$

When the correction factor is incorporated with equation (3):

$$\dot{D}[r,1] = A[1]\left(\frac{\mu_a [hv_{avg}]}{\rho}\right)_{air} (hv)_{avg} \frac{1}{2} \int_{h}^{\infty} \frac{e^{-\left(\mu_t [hv_{avg}]_{air} s\right) - \frac{1}{2}\left(\frac{s^2 - h^2}{\sigma_r^2}\right)}}{s} ds \tag{21}$$

The next step is calculating a reasonable value for σ_r. The following empirical relationship (modified to use variables consistent with this thesis) relates yield to σ_r (Pugh,1959:24):

$$\sigma_r = 1.609 e^{\left[0.70 + \frac{1}{3}\ln(Y) - \frac{3.25}{4.0 + [\ln(Y) + 5.4]^2}\right]} \tag{22}$$

Where,

σ_r represents the standard deviation of the fallout distribution in [km], and

Y is yield in [kilotons].

Using the model values of one kiloton and a detector height of one meter:

$$\sigma_r = 2.9 km = 2900 m$$

Non-Uniform Activity Results

Evaluating equation (22) using an average photon energy of 0.81MeV and including the BUF value of 1.1 obtained in Chapter III, the SNC is calculated to be:

42

$$\boxed{\text{Variable Activity SNC} = 8.6 \times 10^{-16} \left\{ \frac{J - m^2}{kg - \sec - Bq} \right\}}$$

Calculated in *Appendix A,* this value indicates a mere 1.8×10^{-2} % decline in the SNC calculated

in Chapter IV from varying activity[28].

The standard deviation of the fallout distribution is the driving factor in any impact on

the SNC. In other words, the smaller the standard spatial deviation of the fallout distribution,

the steeper the decline in activity density as position is increased from the detector. The

assumption of no wind represented the worst case scenario (or smallest standard deviation).

This means *at worst* the variation in activity density has insignificant impact. Nonetheless,

several calculations were made using a variety of values for standard deviation to further

illustrate the impact on correction factor Figure (21) and SNC (Figure 22).
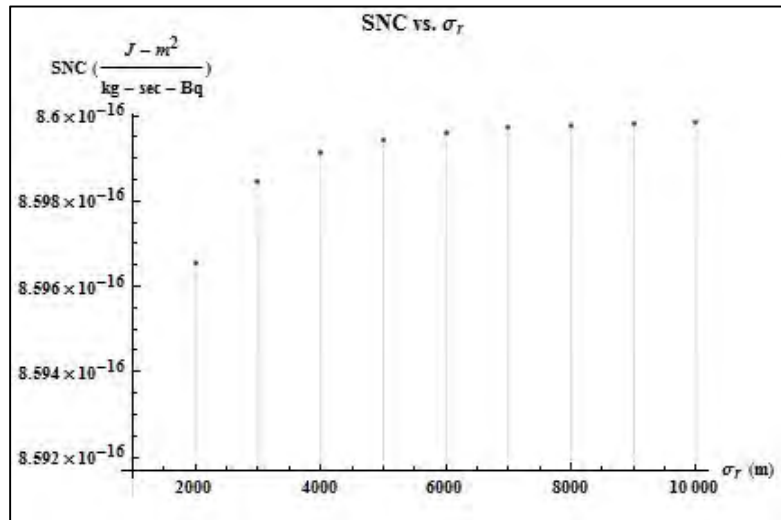
Figure 22. Source Normalization Constant as a function of fallout standard deviation.

---

[28] See *Appendix A* (7)
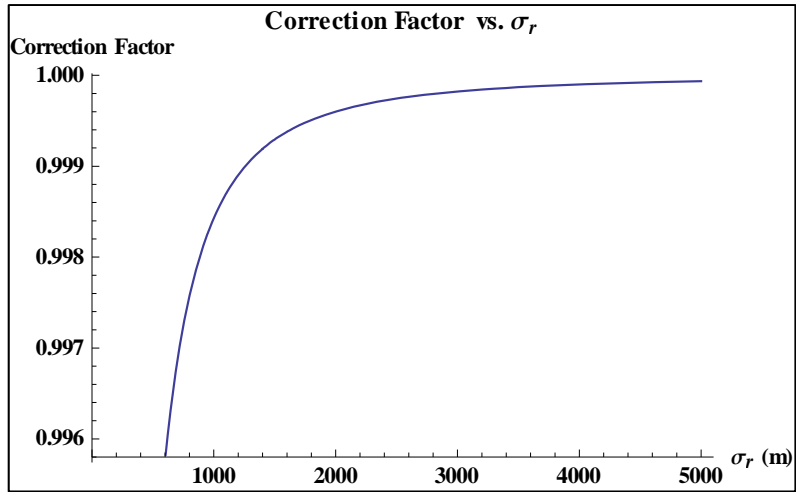
Figure 23. Correction Factor as a function of fallout standard deviation.

Shown in Figures 21 and 22, even as standard deviation is reduced below 1km the correction factor still maintains a value greater than 0.99. Next, the impacts of time on SNC are considered.

VI. The Impact of Time on the Source Normalization Constant

As shown in Chapter III, the BUF has a strong energy dependence. In Chapter IV,

the reduction of the fallout energy distribution to a single average photon energy and an

average BUF is shown to be accurate in calculating the source normalization constant (SNC).

Though as time progresses, the distribution of energy is expected to change as short-lived high

energy emitting isotopes decay into longer-lived lower energy emitting isotopes. This change

in distribution will also affect the average BUF value. In this chapter, we investigate the

impacts of time on calculating the source normalization constant.

The Way-Wigner Approximation

In 1948, Katherine Way and Eugene Wigner published what is known as the Way-

Wigner approximation. In their publication, an extensive theoretical treatment of radioactive

decay yields the relationship (Way, 1948):

$$\dot{D}_{GD}(t) = \dot{D}_{GD}(1)t^{-1.2} \qquad (23)$$

Where,

$\dot{D}_{GD}(t)$ is the dose rate at time t in $\left[\dfrac{J}{kg-\sec}\right]$;

$\dot{D}_{GD}(1)$ is the dose rate at unit time (1hr, 1 day, 1 month) in $\left[\dfrac{J}{kg-\sec}\right]$ and

t is time in whatever units are being used for the unit time value.

Combining equation (23) with an updated version of equation (6) featuring the new SNC at

one hour yields equation (24):

$$\dot{D}[X,Y,t] = 8.6 \times 10^{-16} A[X,Y,1] \ t^{-1.2} \left\{ \frac{J}{kg - \sec} \right\}$$

<div align="right">(24)</div>

This relationship reveals an important distinction in the application of the Way-Wigner approximation which is discussed in the next section.

Time Impact on Source Normalization Constant (1 – 72 Hours)

As shown in equation (24), dose rate is calculated by multiplying an activity density by a source normalization constant. The cumulative impact of time affects both of these factors. Since half-life generally increases as fallout progresses down the decay chain, activity will inherently decline. In fact, this is precisely the effect addressed by the Way-Wigner approximation. Unfortunately, this does not address any impacts on the source normalization constant.

For example, as the activity density changes the distribution of that activity across the energy spectrum also changes. This means the average photon energy for the spectrum will change. As a consequence, this also changes the weight values used to calculate an average BUF for the distribution. The question becomes: are these changes in distribution and energy significant enough to warrant a separate time correction term?

To determine the impact of time on the SNC, runs for 90/10 U-235/U-238 at various times are created within the ORIGEN Fallout Analysis Tool for times of 12 hours, 24 hours, 48 hours, and 72 hours. Identical to the procedure used in Chapter IV, each time interval is analyzed to obtain average photon energy and a weighted distribution function to calculate an

average BUF. A summary of these results is illustrated in Figure 24. A sample of completed code results is included in *Appendix D* for the 12 hour case.
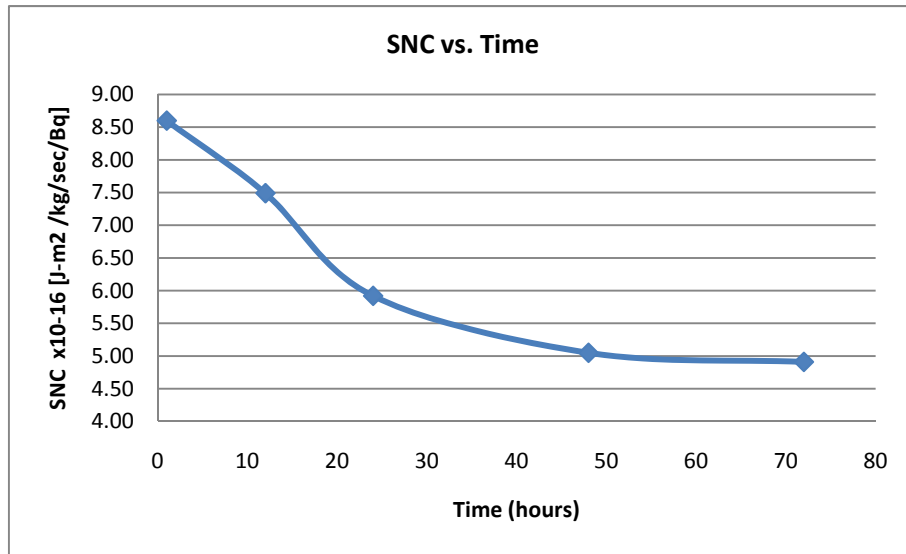
Figure 24. The source normalization constant as a function of time

As shown in Figure 24, the SNC decreases steadily over time. As time increases, the declining average photon energy and the impact of different weight distributions on the average BUF are the most likely causes; however, further analysis is necessary to determine which of these factors drives the decline.

If fallout activity distributions increasingly favor low energies over time, the average BUF value is expected to increase (see Figure 10). This prediction holds true when average BUF values are calculated with weighting factors from the ORIGEN Fallout Analysis Tool (Figure 25). An important observation is the range of increase beginning at 1.1 and rising to a value of 1.2 before 72 hours, representing a 9.0% increase.
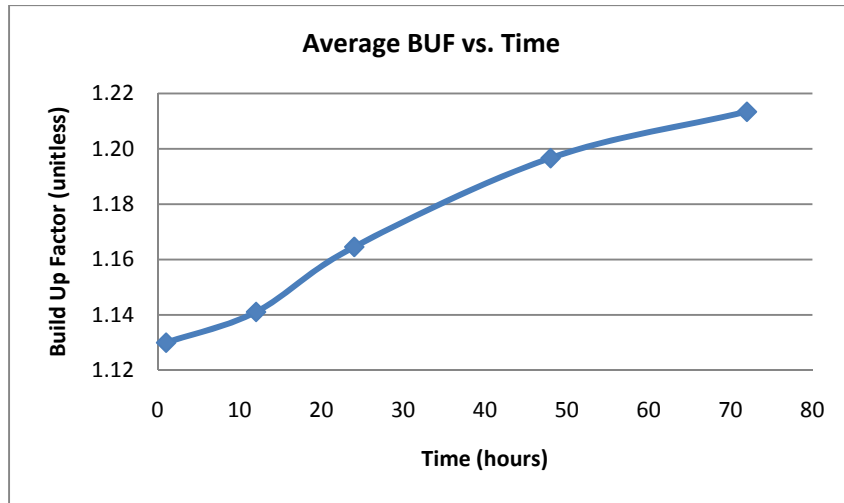
Figure 25. The build up factor as a function of time

As a consequence of the energy distribution initially favoring lower energies as time increases, the average photon energy is also expected to decline. This is verified again by graphing results obtained from the ORIGEN Fallout Analysis Tool (Figure 26).
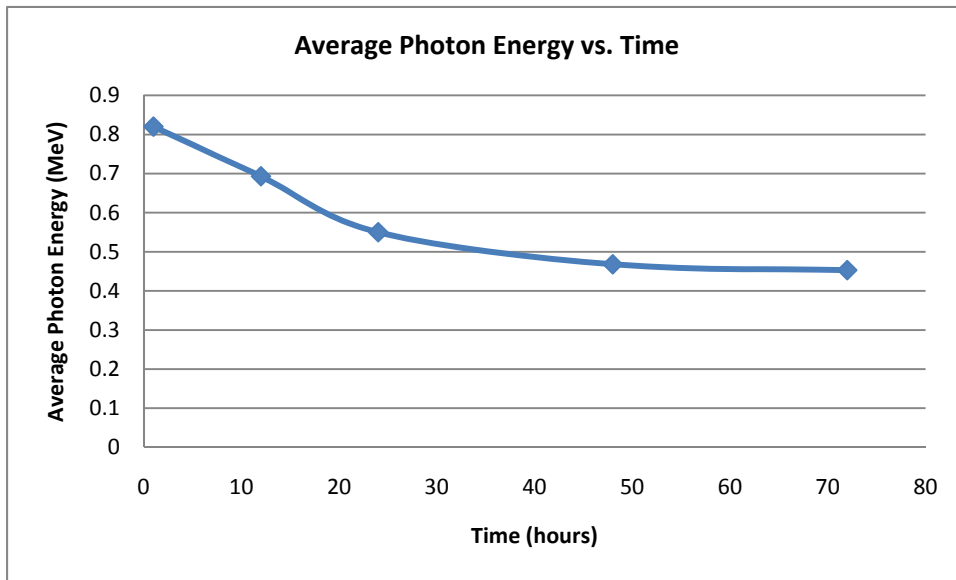
Figure 26. Average photon energy as a function of time

In examining Figure 26, a decline in average energy from 0.81MeV to 0.45MeV is observed over the first 72 hours. This represents a 56% decline, overcoming the effects of increasing BUF values discussed earlier.

Time Impact on Source Normalization Constant (72 Hours – 1 Month)

Figures 24-26 seem to indicate an approach to stable values after 72 hours; however, additional analysis of average BUF and average energy extended out to one month indicates differently. Using the same methods as previously described for 90/10 U-235/U-238 fission, Figures 27-29 show a steady increase in average photon energy, a decrease in average BUF, and an increase of the SNC value:
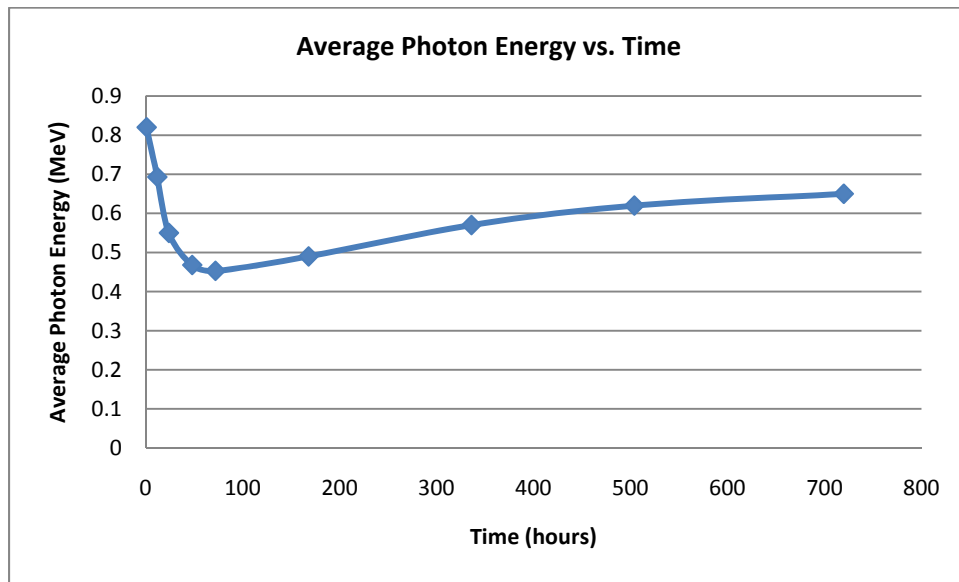
Figure 27. Average Photon Energy as a function of time out to one month.
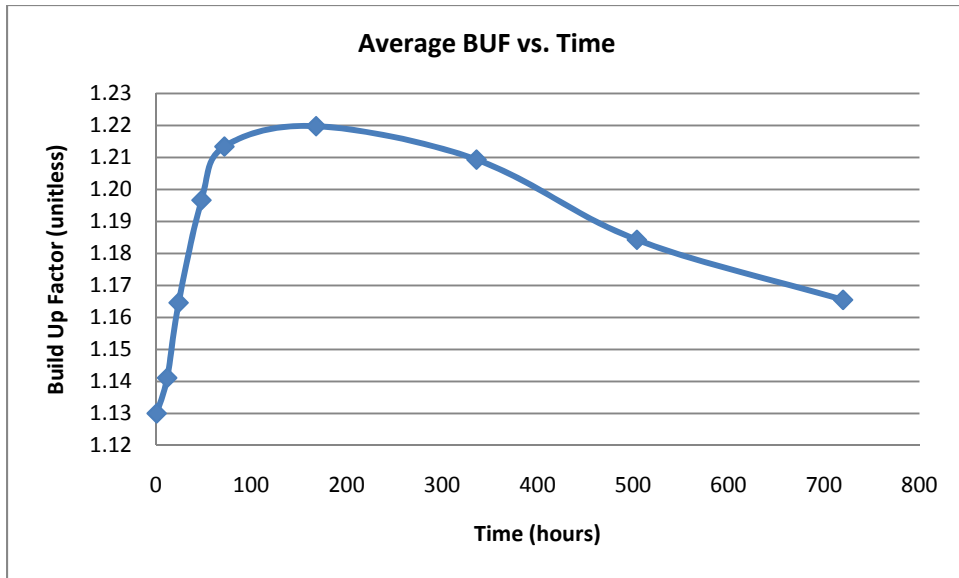
Figure 28. Average Photon Energy as a function of time out to one month.
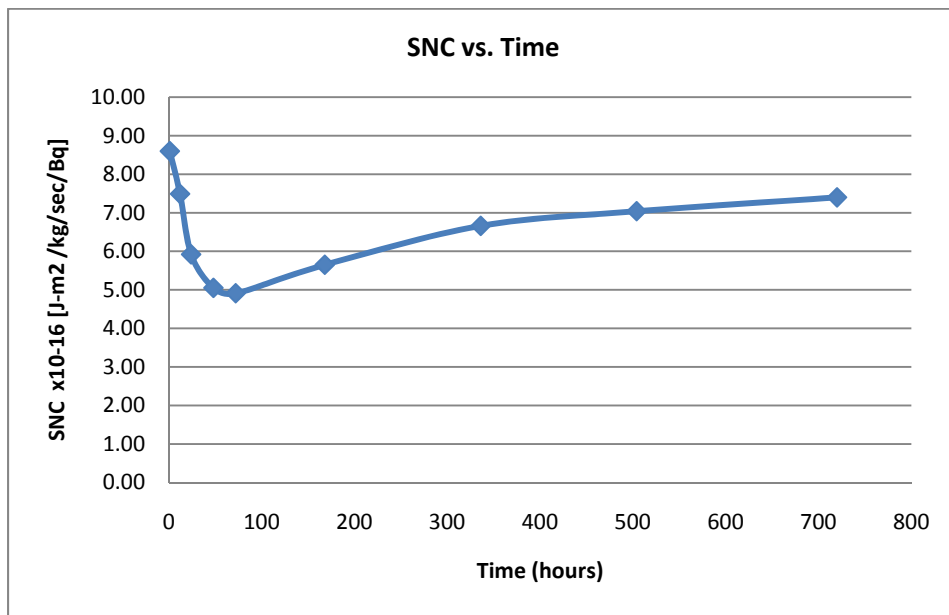
Figure 29. Average Photon Energy as a function of time out to one month.

Using previously described methods, the SNC at one month is:

$$\text{SNC at 1 Month} = 7.4 \times 10^{-16} \left\{ \frac{J - m^2}{kg - \sec - Bq} \right\}$$

Figures 27-29 reinforce the fact that average photon energy is the driving factor in determining the SNC, but what causes the average energy to *increase* after 72 hours?

Although the entire energy distribution varies over time, one isotope in particular is determined to be a major contributor to the increase in both average gamma ray energy and SNC. Consider the decay chain:

$$^{140}Xe \rightarrow {}^{140}Cs \rightarrow {}^{140}Ba \rightarrow {}^{140}La$$
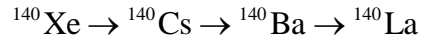
Half-lives for the first three isotopes are 13.6 sec, 1.06 min, 12.75 days, respectively. The half-life of ^{140}La is only 1.68 days, meaning ^{140}La and ^{140}Ba will form a transient equilibrium. Furthermore, ^{140}La emits a 1.60MeV gamma ray compared to a 0.54MeV gamma ray from ^{140}Ba (Baum, 2002:56).

According to the ORIGEN Fallout Analysis Tool, the energy contribution of ^{140}La at a time of 72 hours is 2.6% of the entire fallout energy distribution[29]. As time increases, the contribution of ^{140}La also continues to increase. At two weeks, ^{140}La accounts for 13%. At one month, ^{140}La accounts for 16%. Although several other decay chains influence the average gamma ray energy, these results suggest ^{140}La is a major contributor. Using Figure 27 and 29 as a reference, the initial decline in average gamma ray energy (and SNC) can be viewed as a lack of ^{140}La present. After a few days, ^{140}Ba begins to decay into ^{140}La. The comparatively short half-life of 1.68 days coupled with the 1.6MeV gamma ray emission of ^{140}La pushes the average gamma ray energy back up to 0.65MeV, thereby increasing the SNC to the aforementioned value.

---

[29] See *Appendix C*

VII. Conclusions and Recommendations

As previously stated, the objective of this research was to analyze the assumptions listed in Chapter I regarding the first order model developed to calculate dose rate of a detector positioned one meter above a fallout field. As the assumptions were relaxed, any quantitative impacts were combined to form an updated source normalization constant.

In Chapters II and III, assumption #1 of "no scattering" was partially relaxed by utilizing an integral method of successive scatters. By including one scatter and a limited second scatter approximation, the build up factor (BUF) was determined to be 1.1 for an average photon energy of 0.70MeV. This result indicates scattering contributes an additional 10% to dose rate.

In analyzing BUF values for energies other than 0.70MeV, it became apparent that the BUF changes significantly over the energy spectrum – most notably to a value of 1.9 at 0.02MeV. Since the location of this BUF peak is an artifact of only considering a single scatter, further research into multiple scatters is highly recommended. A Monte-Carlo scheme would be best suited in this endeavor.

Since the BUF was shown to carry significant energy dependence, the assumption of using a single average photon energy to represent the full fallout energy distribution was addressed next. In Chapter IV, individual BUF values were assigned to energy groups spanning the range of 0.0MeV to 3.5MeV. Using the ORIGEN Fallout Analysis Tool provided by Oak Ridge National Laboratory, weighted values for the fallout energy distribution were obtained for each energy group and used to calculate a weighted BUF average. The result of this effort was a confirmation of a BUF value of 1.1.

Over the course of determining an average BUF value, it was shown by the ORIGEN Fallout Analysis Tool that the average photon energy of a fallout field at one hour is 0.81MeV – in contrast with the widely accepted value of 0.70MeV listed in *The Effects of Nuclear Weapons* (Glasstone, 1977:454). Using the new average photon energy and average BUF value, a refined source normalization constant at one hour was determined to be:

$$8.6 \times 10^{-16} \left\{ \frac{J - m^2}{kg - \sec - Bq} \right\}$$

In comparing this SNC with one calculated using a multi-group approach, it was determined that fallout distributions can be modeled using a single average photon energy in conjunction with a weighted average BUF term. This was proven by identical SNC values calculated with the two methods.

Chapter V explored the impact of non-uniform activity across a fallout field. Using a normalized Gaussian distribution to model a no wind (worst case) scenario, less than a 1.8×10^{-2} % decline was observed on the SNC. Further analysis of standard deviations from 1000m to 10,000m showed the impacts of standard deviation on the SNC and correction factor, confirming the result that assuming uniform activity density (assumption #4) determined by the activity density directly beneath the detector yields an accurate approximation of SNC within a fraction of a percent.

In Chapter VI, the effects of time (assumption #3) were explored to determine if a separate time correction factor was needed to address the changes in energy distributions that compose SNC and BUF values. After analyzing the effects of time on SNC, a separate time correction factor was found to be necessary to adjust the SNC at times other than one hour. This was determined by discovering a sudden 57% decline in SNC over the first 72 hours,

followed by an increase to 86% of its original value after one month. This result indicates assumption #3 is not sufficient in modeling the effects of time on dose rate and an additional time correction factor for the SNC is required.

Furthermore, ^{140}La is determined to be a major contributor to the increase in average gamma ray energy and SNC at times greater than 72 hours. Using the ORIGEN Fallout Analysis Tool, the energy contribution of ^{140}La is shown to increase from 2.8% to 16% of the fallout energy distribution by the end of the first month. This large contribution coupled with the 1.6MeV gamma ray emission of ^{140}La drives the average gamma ray energy and SNC to increase after 72 hours.

Finally, the assumption of ground as a smooth and level plane has already been addressed in *The Self-Shielding of Fallout Gamma Rays by Terrain Roughness* by Herte. Using a Monte-Carlo code (MORSE) to model surface roughness, his results indicate self-shielding between 2-5% for soil. This value is shown to vary significantly based on surface type, so its effects are not incorporated into the final SNC value.

Although several aspects regarding the SNC were analyzed, several assumptions are left outstanding. As previously mentioned, this analysis addresses only one scatter and a limited approximation of second scatter. Table 1 demonstrates the impact of this limitation.

Table 1. Flight-by-Flight Average Photon Energies

Flight	Incident Energy (MeV)	Average Post Scatter energy (MeV)	Mean Free Path in Air (m)
0	0.70	0.38	109
1	0.38	0.25	83
2	0.25	0.18	72
3	0.18	0.14	67
4	0.14	0.11	59
5	0.11	0.093	57
6	0.093	0.078	52
7	0.078	0.070	48
8	0.070	0.062	46

As shown in Table 1, average photon energy decreases an order of magnitude after 8 scatters, but mean free path is only reduced 42%. This result strongly indicates that modeling many scatters is necessary to refine the BUF term. Furthermore, most of the analyzed scatters were assumed to be isotropic – clearly disproven by Klein-Nishina. While certain approximations made rough adjustments to correct for non-isotropic scatter, a more in-depth analysis may show further impact to the BUF term.

<center>*A p p e n d i x   A*
Supporting calculations</center>

(1) <u>Post-Scatter energy for 0.70MeV:</u>

   Using equations from *The Atomic Nucleus* (Evans, 675), the relationship between

incident photon energy, scattering angle, and post-scatter energy is defined:

$$\frac{hv'}{hv_0} = \frac{1}{1+\alpha(1-\cos\vartheta)}$$

$$\alpha = \frac{hv_0}{m_0 c^2}$$

As discussed in Chapter II a weighted average is used to determine the average scattering angle

$\bar{\vartheta}$.

$$\bar{\vartheta} = \frac{\int_0^\pi \frac{r_0^2}{2}\left(\frac{hv'}{hv_0}\right)^2\left[\left(\frac{hv_0}{hv'}\right)^2 + \left(\frac{hv'}{hv_0}\right) - \sin^2\vartheta\right]\vartheta\, d\vartheta}{\int_0^\pi \frac{r_0^2}{2}\left(\frac{hv'}{hv_0}\right)^2\left[\left(\frac{hv_0}{hv'}\right)^2 + \left(\frac{hv'}{hv_0}\right) - \sin^2\vartheta\right] d\vartheta} = 1.17 \text{ radians}$$

This average scattering angle is then used in equation (16) to find average post-scatter energy:

$$hv' = \frac{1}{1+\alpha(1-\cos\bar{\vartheta})} hv_0 = 0.38 MeV$$

The Mathematica script for this calculation is:

```
NIntegrate[(2.81794*10^-15)^2/2 * (ER[⊙])^2 * (ER[⊙]^-1 + ER[⊙] - Sin[⊙]^2) 2 π * Sin[⊙] * ⊙, {⊙, 0, π}]/
NIntegrate[(2.81794*10^-15)^2/2 * (ER[⊙])^2 * (ER[⊙]^-1 + ER[⊙] - Sin[⊙]^2) 2 π * Sin[⊙], {⊙, 0, π}]

1.17366

1/(1 + α * (1 - Cos[%])) * hv0

0.380429
```

<center>56</center>

(2) <u>Second Flight (1st scatter) contribution to the detector of 7.5%:</u>

Several constants are required for this calculation, starting with the incident energy and average

first/second scatter energies:

$$hv_0 = 0.70MeV$$
$$hv' = 0.38MeV$$
$$hv'' = 0.25MeV$$

The cross sections used for this calculation are:

For Air:
$$\begin{cases} \mu_s^o = 9.2 \times 10^{-3} \left\{ m^{-1} \right\} \\ \mu_s' = 1.2 \times 10^{-2} \left\{ m^{-1} \right\} \\ \mu_s'' = 1.4 \times 10^{-2} \left\{ m^{-1} \right\} \\ \mu_a^o = 9.9 \times 10^{-7} \left\{ m^{-1} \right\} \\ \mu_a' = 4.9 \times 10^{-6} \left\{ m^{-1} \right\} \\ \mu_a'' = 1.7 \times 10^{-5} \left\{ m^{-1} \right\} \\ \mu_t^o = 9.2 \times 10^{-3} \left\{ m^{-1} \right\} \\ \mu_t' = 1.2 \times 10^{-2} \left\{ m^{-1} \right\} \\ \mu_t'' = 1.4 \times 10^{-2} \left\{ m^{-1} \right\} \end{cases}$$

For Ground:
$$\begin{cases} \mu_s^o = 13 \left\{ m^{-1} \right\} \\ \mu_s' = 17 \left\{ m^{-1} \right\} \\ \mu_a^o = 7.1 \times 10^{-3} \left\{ m^{-1} \right\} \\ \mu_a' = 3.5 \times 10^{-2} \left\{ m^{-1} \right\} \\ \mu_t^o = 13 \left\{ m^{-1} \right\} \\ \mu_t' = 17 \left\{ m^{-1} \right\} \end{cases}$$

As previously stated, density for ground and air are taken as:

$$\text{Air: } \rho = 1.23 \left\{ \frac{kg}{m^3} \right\}$$
$$\text{Ground: } \rho = 1900 \left\{ \frac{kg}{m^3} \right\}$$

Evaluating equation (12) from Chapter II yields a value of isotropic air scatter contribution to

the detector:

$$\dot{D}_{SF}^{air} = C\left[\int_0^h E_1\left[\mu_t^o(h-u)\right]E_1\left[\mu_t'u\right]du + \int_0^\infty E_1\left[\mu_t^o(w+h)\right]E_1\left[\mu_t'w\right]dw\right] = A_{gd}\,5.9\times10^{-17}\left\{\frac{J}{kg-\sec}\right\}$$

```
Dose1SA = 1/4 * hv1 * ( (AMuA1 + σₐ[hv1]) / ARoe ) * Agd * MeVtoJ * AMuS0 *
   (NIntegrate[F[AMuT0 (1 - x)] * F[AMuT1 * (x)], {x, 0, 1}, WorkingPrecision → 10] +
      NIntegrate[F[AMuT0 (w + 1)] * F[AMuT1 * (w)], {w, 0, Infinity}, WorkingPrecision → 10])
5.85205 × 10⁻¹⁷
```

Likewise for ground contribution, evaluating equation (15) yields a value of isotropic ground

scatter contribution to the detector:

$$\dot{D}_{SF}^{gd} = C\int_h^\infty E_1\left[\left(\mu_t^o\right)_{gd}(u-h)\right]E_1\left[\left(\mu_t'\right)_{gd}(u-h)+\left(\mu_t'\right)_{air}h\right]du = A_{gd}\,4.8\times10^{-17}\left\{\frac{J}{kg-\sec}\right\}$$

```
Dose1SG = 1/4 * MeVtoJ * hv1 * ( (AMuA1 + σₐ[hv1]) / ARoe ) * Agd * GMuS0 *
   NIntegrate[F[GMuT0 (x - 1)] * F[(GMuT1 * (x - 1)) + (AMuT1)], {x, 1, Infinity}, WorkingPrecision → 10]|
4.80302 × 10⁻¹⁷
```

Combined with the evaluated value of direct flight (DF) contribution in equation (4):

$$\dot{D}_{DF} = A_{gd}\,6.8\times10^{-16}\left[\frac{J}{kg-\sec}\right]$$

```
DoseDF = 1/2 * hv0 * MeVtoJ * Agd * ( (AMuA0 + σₐ[hv0]) / ARoe ) * F[AMuT0]
6.75885 × 10⁻¹⁶
```

The total dose rate is the sum of these three values. Various percentage based contributions

can be calculated from these values. For example:

$$\frac{\dot{D}_{SF}^{air}}{\dot{D}_{SF}^{air}+\dot{D}_{SF}^{gd}+\dot{D}_{DF}} = \%\ \text{Air Scatter Contribution} = 7.5\%$$

$$\frac{\dot{D}_{SF}^{gd}}{\dot{D}_{SF}^{air}+\dot{D}_{SF}^{gd}+\dot{D}_{DF}} = \%\ \text{Ground Scatter Contribution} = 6.1\%$$

58

$$\frac{\text{Dose1SA}}{(\text{Dose1SA} + \text{Dose1SG} + \text{DoseDF})} * 100 \qquad \frac{\text{Dose1SG}}{(\text{Dose1SA} + \text{Dose1SG} + \text{DoseDF})} * 100$$

$$7.47927 \qquad\qquad\qquad\qquad\qquad\qquad 6.13855$$

(3) <u>The contribution of air scatter coming from the region above the detector:</u>

Evaluating equations (10) and (11) yield the dose rate contributions from air scatter received from below and above the detector (respectively). When combined, these regions become the total contribution of air scatter to the detector equation (12). Using the constant value obtained from equation (12) as the total dose rate, the percentage contributions from the region above or below the detector can be calculated.

For Region II (Below): $\displaystyle \dot{D}_{SF(II)}^{air} = C\left[\int_0^h \left(\int_{h'}^{\infty} \frac{e^{-(\mu_t^o)_{air} s'}}{s'} ds' + \int_{h-h'}^{\infty} \frac{e^{-(\mu_t')_{air} s''}}{s''} ds'' \right) dh' \right]$

For Region III (Above): $\displaystyle \dot{D}_{SF(III)}^{air} = C\left[\int_h^{\infty} \left(\int_{h'}^{\infty} \frac{e^{-(\mu_t^o)_{air} s'}}{s'} ds' + \int_{h'-h}^{\infty} \frac{e^{-(\mu_t')_{air} s''}}{s''} ds'' \right) dh' \right]$

Combine Region II and III for total air contribution:

$$\dot{D}_{SF}^{air} = C\left[\int_0^h E_1\left[\mu_t^o(h-u) \right] E_1\left[\mu_t' u \right] du + \int_0^{\infty} E_1\left[\mu_t^o(w+h) \right] E_1\left[\mu_t' w \right] dw \right]$$

The percent contribution coming from Region III (Above) is then:

$$\frac{\dot{D}_{SF(III)}^{air}}{\dot{D}_{SF}^{air}} = 83\%$$

```
NIntegrate[F[AMuT0 (w + 1)] * F[AMuT1 (w)], {w, 0, Infinity}, WorkingPrecision → 10] /
  (NIntegrate[F[AMuT0 (1 - x)] * F[AMuT1 (x)], {x, 0, 1}, WorkingPrecision → 10] +
     NIntegrate[F[AMuT0 (w + 1)] * F[AMuT1 (w)], {w, 0, Infinity}, WorkingPrecision → 10]) * 100

82.9597249
```

(4) <u>The BUF of 1.1 for average incident energy of 0.70MeV:</u>

This value was obtained using equation (18) of Chapter 2. As shown below, equation (18) was

modified to include the Ground Non-isotropic Adjustment Term.

$$GNAT = \frac{\int_{\frac{\pi}{2}}^{\frac{3\pi}{2}} \frac{r_0^2}{2}\left(\frac{hv'}{hv_0}\right)^3\left[\left(\frac{hv_0}{hv'}\right)+\left(\frac{hv'}{hv_0}\right)-\sin^2\vartheta\right]d\vartheta}{\int_0^{2\pi} \frac{r_0^2}{2}\left(\frac{hv'}{hv_0}\right)^3\left[\left(\frac{hv_0}{hv'}\right)+\left(\frac{hv'}{hv_0}\right)-\sin^2\vartheta\right]d\vartheta} = 0.10$$

```
GNAT = NIntegrate[ (2.81794 * 10^-15)^2 / 2 * (ER[θ])^3 * (ER[θ]^-1 + ER[θ] - Sin[θ]^2), {θ, π/2, 3π/2}] /

    NIntegrate[ (2.81794 * 10^-15)^2 / 2 * (ER[θ])^3 * (ER[θ]^-1 + ER[θ] - Sin[θ]^2), {θ, 0, 2π}]

0.0992015
```

This term was used to determine the fraction for ground scatter near the detector that was able

to scatter back into the air. From this value, a limited second scatter approximation (LSSA)

was made.

$$\dot{D}_{LSSA} = GNAT \times \frac{1}{4} hv''\left(\frac{\mu_a''}{\rho}\right)_{air} A_{gd}\left(\mu_s'\right)_{air}\left[\int_0^1 E_1\left[\mu_t'(1-u)\right]E_1\left[\mu_t''(u)\right]du + \int_0^\infty E_1\left[\mu_t'(w+1)\right]E_1\left[\mu_t''(w)\right]dw\right]$$

$$\dot{D}_{LSSA} = A_{gd}\,3.9\times10^{-18}\left\{\frac{J}{kg-\sec}\right\}$$

```
Dose1SA1SG = GNAT * 1/4 * MeVtoJ * hv2 * ( (AMuA2 + σa[hv2]) / ARoe ) * Agd * AMuS1 *

    (NIntegrate[F[AMuT1 (1 - x)] * F[AMuT2 (x)], {x, 0, 1}, WorkingPrecision → 6] +

        NIntegrate[F[AMuT1 (w + 1)] * F[AMuT2 (w)], {w, 0, Infinity}, WorkingPrecision → 6])

3.87647 × 10^-18
```

Combining these values with previously calculated values for air and ground contributions, the

BUF is calculated using equation (18):

$$BUF = 1 + \frac{\dot{D}_{SF}^{air} + \left(GNAT \times \dot{D}_{SF}^{gd}\right) + \dot{D}_{LSSA}}{\dot{D}_{DF}} = 1.1$$

(5) Calculating Mean Free Path:

Calculating the mean free path for a photon is simply the inverse of its macroscopic cross section for attenuation. For a 0.02MeV gamma ray in air:

$$\mu_t = 5.5 \times 10^{-2} \left\{m^{-1}\right\}$$

$$\frac{1}{\mu_t} = 18 \left\{m\right\}$$

For a 0.70MeV gamma ray in air:

$$\mu_t = 9.2 \times 10^{-3} \left\{m^{-1}\right\}$$

$$\frac{1}{\mu_t} = 109 \left\{m\right\}$$

For a 0.02MeV gamma ray in ground:

$$\mu_t = 475.5 \left\{m^{-1}\right\}$$

$$\frac{1}{\mu_t} = 2.1 \times 10^{-3} \left\{m\right\}$$

For a 0.70MeV gamma ray in ground:

$$\mu_t = 12.8 \left\{m^{-1}\right\}$$

$$\frac{1}{\mu_t} = 7.8 \times 10^{-2} \left\{m\right\}$$

(6) Calculations involving average energy of 0.81MeV:

Several constants are required for this calculation, starting with the incident energy and average first/second scatter energies:

$$hv_0 = 0.81 MeV$$
$$hv' = 0.413 MeV$$
$$hv'' = 0.267 MeV$$

The cross sections used for this calculation are:

For Air:
$$\begin{cases}
\mu_s^o = 8.661 \times 10^{-3} \{m^{-1}\} \\
\mu_s' = 1.154 \times 10^{-2} \{m^{-1}\} \\
\mu_s'' = 1.365 \times 10^{-2} \{m^{-1}\} \\
\mu_a^o = 7.167 \times 10^{-7} \{m^{-1}\} \\
\mu_a' = 3.850 \times 10^{-6} \{m^{-1}\} \\
\mu_a'' = 1.415 \times 10^{-5} \{m^{-1}\} \\
\mu_t^o = 8.64 \times 10^{-3} \{m^{-1}\} \\
\mu_t' = 1.15 \times 10^{-2} \{m^{-1}\} \\
\mu_t'' = 1.36 \times 10^{-2} \{m^{-1}\}
\end{cases}$$

For Ground:
$$\begin{cases}
\mu_s^o = 12.02 \{m^{-1}\} \\
\mu_s' = 16.01 \{m^{-1}\} \\
\mu_a^o = 5.116 \times 10^{-3} \{m^{-1}\} \\
\mu_a' = 2.752 \times 10^{-2} \{m^{-1}\} \\
\mu_t^o = 12.02 \{m^{-1}\} \\
\mu_t' = 16.05 \{m^{-1}\}
\end{cases}$$

As previously stated, density for ground and air are taken as:

$$\text{Air: } \rho = 1.23 \left\{ \frac{kg}{m^3} \right\}$$

$$\text{Ground: } \rho = 1900 \left\{ \frac{kg}{m^3} \right\}$$

Evaluating equation (12) from Chapter II yields a value of isotropic air scatter contribution to the detector:

$$\dot{D}_{SF}^{air} = C \left[\int_0^h E_1 \left[\mu_t^o (h-u) \right] E_1 \left[\mu_t' u \right] du + \int_0^\infty E_1 \left[\mu_t^o (w+h) \right] E_1 \left[\mu_t' w \right] dw \right] = A_{gd} 6.2 \times 10^{-17} \left\{ \frac{J}{kg - \sec} \right\}$$

```
Dose1SA = 1/4 * hv1 * ( (AMuA1 + σ_a [hv0]) / ARoe ) * Agd * MeVtoJ * AMuS0 *
    (NIntegrate[F[AMuT0 (1 - x)] * F[AMuT1 (x)], {x, 0, 1}, WorkingPrecision → 10] +
        NIntegrate[F[AMuT0 (w + 1)] * F[AMuT1 (w)], {w, 0, Infinity}, WorkingPrecision → 10])

6.15055 × 10^-17
```

Likewise for ground contribution, evaluating equation (15) yields a value of isotropic ground scatter contribution to the detector:

$$\dot{D}_{SF}^{gd} = C\int_{h}^{\infty} E_1\left[\left(\mu_t^o\right)_{gd}(u-h)\right]E_1\left[\left(\mu_t'\right)_{gd}(u-h)+\left(\mu_t'\right)_{air}h\right]du = A_{gd}\,5.1\times10^{-17}\left\{\frac{J}{kg-\sec}\right\}$$

```
Dose1SG = 1/4 * MeVtoJ * hv1 * ( (AMuA1 + σ_a [hv0]) / ARoe ) * Agd * GMuS0 *
    NIntegrate[F[GMuT0 (x - 1)] * F[(GMuT1 * (x - 1)) + (AMuT1)], {x, 1, Infinity}, WorkingPrecision → 10]
5.07239 × 10^-17
```

Combined with the evaluated value of direct flight (DF) contribution in equation (4):

$$\dot{D}_{DF} = A_{gd}\,7.7\times10^{-16}\left[\frac{J}{kg-\sec}\right]$$

```
DoseDF = 1/2 * hv0 * MeVtoJ * Agd * ( (AMuA0 + σ_a [hv0]) / ARoe ) * F[AMuT0]
7.73314 × 10^-16
```

This value was obtained using equation (18) of Chapter 2. As shown below, equation (18) was modified to include the Ground Non-isotropic Adjustment Term.

$$GNAT = \frac{\displaystyle\int_{\frac{\pi}{2}}^{\frac{3\pi}{2}} \frac{r_0^2}{2}\left(\frac{hv'}{hv_0}\right)^3\left[\left(\frac{hv_0}{hv'}\right)+\left(\frac{hv'}{hv_0}\right)-\sin^2\vartheta\right]d\vartheta}{\displaystyle\int_{0}^{2\pi} \frac{r_0^2}{2}\left(\frac{hv'}{hv_0}\right)^3\left[\left(\frac{hv_0}{hv'}\right)+\left(\frac{hv'}{hv_0}\right)-\sin^2\vartheta\right]d\vartheta} = 0.10$$

```
GNAT = NIntegrate[ (2.81794 * 10^-15)^2 / 2 * (ER[θ])^3 * (ER[θ]^-1 + ER[θ] - Sin[θ]^2), {θ, π/2, 3π/2}] /
    NIntegrate[ (2.81794 * 10^-15)^2 / 2 * (ER[θ])^3 * (ER[θ]^-1 + ER[θ] - Sin[θ]^2), {θ, 0, 2π}]
0.0875075
```

This term was used to determine the fraction for ground scatter near the detector that was able to scatter back into the air. From this value, a limited second scatter approximation (LSSA) was made.

$$\dot{D}_{LSSA} = GNAT \times \frac{1}{4} hv'' \left(\frac{\mu_a''}{\rho}\right)_{air} A_{gd} \left(\mu_s'\right)_{air} \left[\int_0^1 E_1\left[\mu_t'(1-u)\right] E_1\left[\mu_t''(u)\right] du + \int_0^\infty E_1\left[\mu_t'(w+1)\right] E_1\left[\mu_t''(w)\right] dw\right]$$

$$\dot{D}_{LSSA} = A_{gd}\, 3.9 \times 10^{-18} \left\{\frac{J}{kg-\sec}\right\}$$

```
Dose1SA1SG = GNAT * 1/4 * MeVtoJ * hv2 * ( (AMuA2 + σₐ[hv1]) / ARoe ) * Agd * AMuS1 *
    (NIntegrate[F[AMuT1 (1 - x)] * F[AMuT2 (x)], {x, 0, 1}, WorkingPrecision → 6] +
     NIntegrate[F[AMuT1 (w + 1)] * F[AMuT2 (w)], {w, 0, Infinity}, WorkingPrecision → 6])

3.82763 × 10⁻¹⁸
```

Combining these values with previously calculated values for air and ground contributions, the BUF is calculated using equation (18):

$$BUF = 1 + \frac{\dot{D}_{SF}^{air} + \left(GNAT \times \dot{D}_{SF}^{gd}\right) + \dot{D}_{LSSA}}{\dot{D}_{DF}} = 1.1$$

Using the average BUF and direct flight dose rate calculated above (with an assumed activity density of 1 {Bq/m²} to yield SNC) results in:

```
SNC = DoseDF * 1.1

8.59999 × 10⁻¹⁶
```

(7) The Impact of Varying Activity Density on SNC

In Chapter V, a correction factor for varying activity density is defined as:

$$\text{Correction Factor} = \frac{\displaystyle\int_h^\infty \frac{e^{-\left(\mu_t[hv_{avg}]_{air}\, s\right)} e^{-\frac{1}{2}\left(\frac{s^2-h^2}{\sigma_r^2}\right)}}{s}\,ds}{\displaystyle\int_h^\infty \frac{e^{-\left(\mu_t[hv_{avg}]_{air}\, s\right)}}{s}\,ds}$$

64

Incorporating this correction factor into equation (3) yields:

$$\dot{D}[r,1] = A[1]\left(\frac{\mu_a[hv_{avg}]}{\rho}\right)_{air} (hv)_{avg} \frac{1}{2}\int_h^\infty \frac{e^{-\left(\mu_t[hv_{avg}]_{air}s\right)}e^{-\frac{1}{2}\left(\frac{s^2-h^2}{\sigma_r^2}\right)}}{s}ds$$

Where $e^{-\frac{1}{2}\left(\frac{s^2-h^2}{\sigma_r^2}\right)}$ is the correction factor for varying activity density. As shown in previous

calculations, the SNC without the correction factor is:

SNC $= \frac{1}{2}$ * hv0 * MeVtoJ * Agd * $\left(\dfrac{(\text{AMuA0} + \sigma_a\,[\text{hv0}])}{\text{ARoe}}\right)$ * F[AMuT0] * BUF

8.59999×10^{-16} Agd

When the correction factor is incorporated into this function, the result is:

SNC $= \frac{1}{2}$ * hv0 * MeVtoJ * Agd * $\left(\dfrac{(\text{AMuA0} + \sigma_a\,[\text{hv0}])}{\text{ARoe}}\right)$ * BUF $\displaystyle\int_1^\infty \dfrac{e^{-(\text{AMuT0}*s)-.5\left(\frac{s^2-1}{\sigma_r^2}\right)}}{s}$ ds // N

8.5984×10^{-16} Agd

The change in SNC is calculated by:

(1 - (8.5984*^-16 / 8.59999*^-16)) * 100

0.0184884

$$\Delta SNC = 1.8\times10^{-2}\%$$

ORIGEN Fallout Analysis Tool Parameters

We begin with opening the Fallout Analysis Tool. The User Interface (UI) should

look like Figure 30 below:
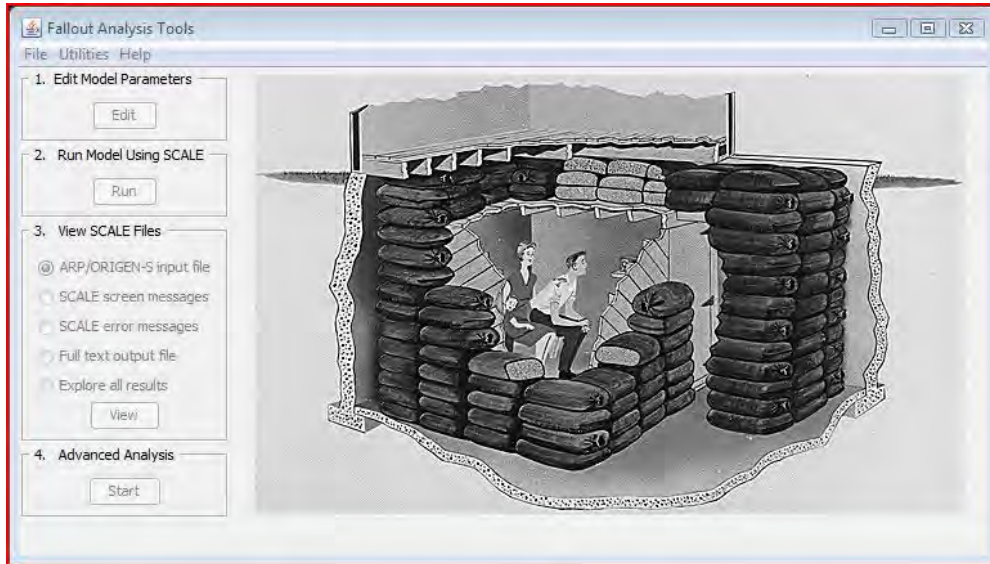
Figure 30. The ORIGEN Fallout Analysis Tool User Interface

Under "File" on the toolbar, select "New." This will open another screen allowing the user to

edit various parameters about the model. In Figure 31, the parameters for the 90%/10% U-

235/U-238 fission are used.

66
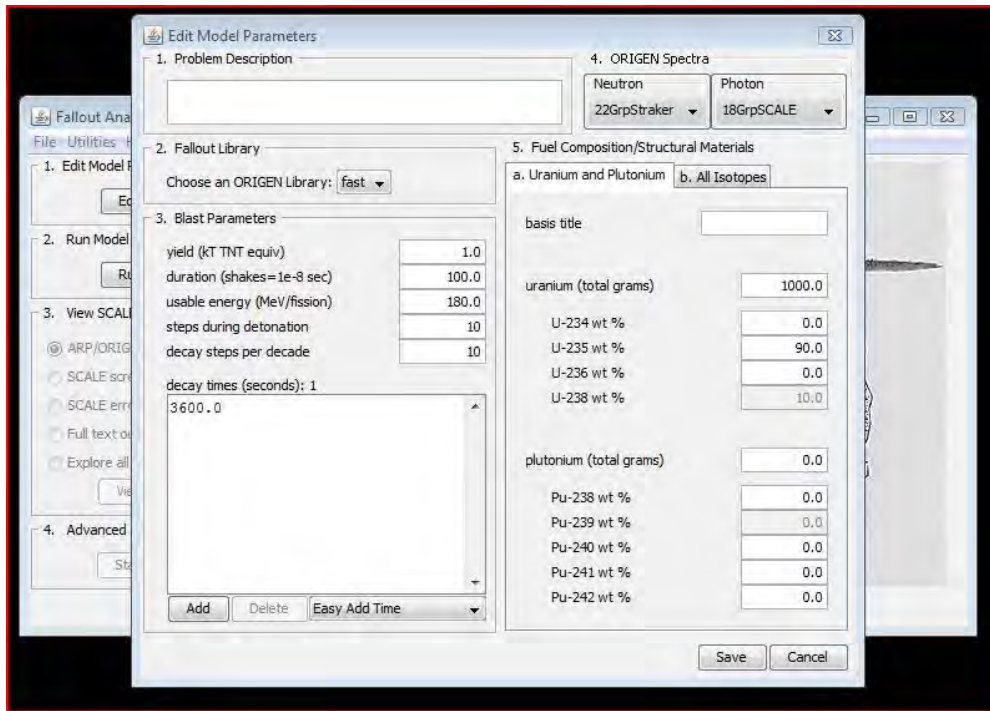
Figure 31. ORIGEN Fallout Analysis Tool Parameters

As shown in Figure 31, a 1.0KT yield with a total mass of 1.0kg is used in this simulation. The values for duration, usable energy per fission, steps during detonation and decay steps per decade are all default values, but may be altered if desired.

The "decay times" block allows the user to input various times of interest to focus analysis. Common denominations such as 1 hour, 1 day, or 1 week may be added using the "Easy Add Time" dropdown menu. Times can also be manually added (in seconds) using the "Add" button on the bottom of the block. Once all parameters are saved, the user is returned to the main UI. From the Main UI, the user now selects the "Run" button in block 2. After 10 – 20 seconds, new options will become available under block 3, "View Scale Files.

Select "Explore all results" and click view at the bottom of the block. This opens an analysis UI with several useful features. For purposes of this research, the user should select

the case time in which they are interested (3600 seconds), select "Export" from the toolbar, and then "Photon Source." (Figure 32)
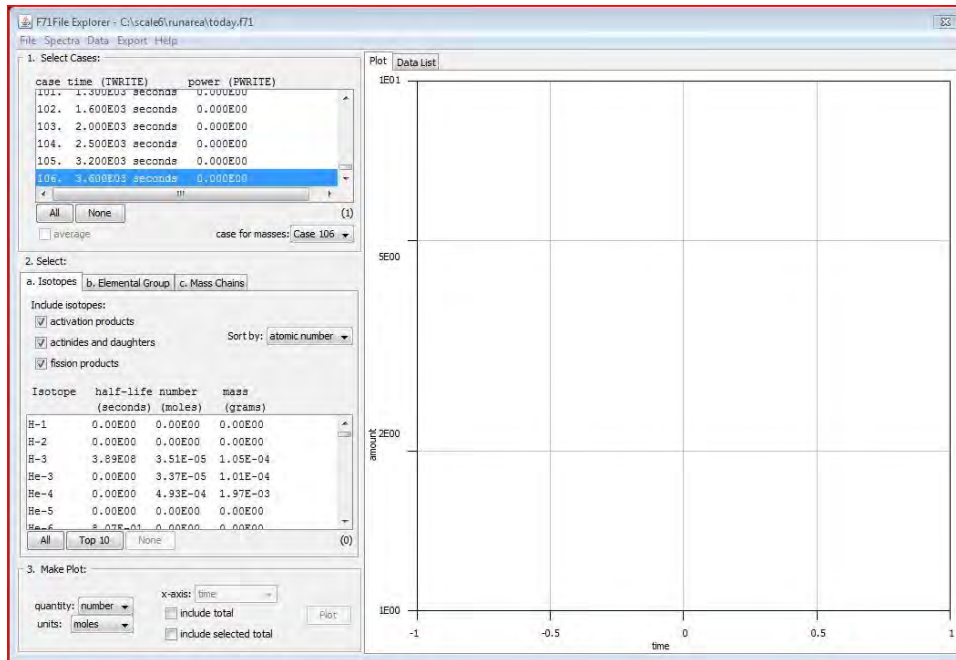
Figure 32. The File Explorer

Once selected, the export photon source option with display the final UI screen allowing the user to specify various parameters. The parameters used for the research contained within this document are illustrated in Figure 32. Once listed, the user selects the "compute" button at the bottom of the interface.
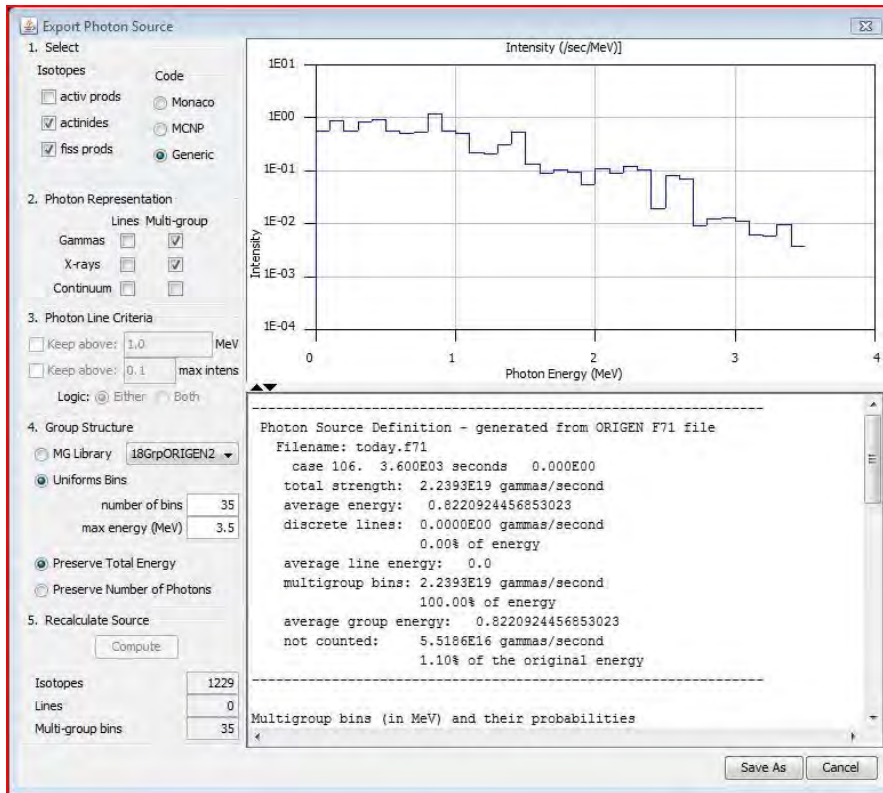
Figure 33. The Export Photon Source UI

Once computed, a plot and a text file will be generated and may be saved if desired. As shown in Figure 33, the average energy for 90/10 fission at a time of 1 hour is 0.82MeV. Also useful is the "not counted" line which gives the total activity and percent of original energy not contained within the user specified energy range. For example, the range of 0.0 – 3.5MeV contains roughly 99% of the entire spectrum.

69

```
100% Pu-239 at 1 Hour
-------------------------------------------------------------
 Photon Source Definition - generated from ORIGEN F71 file
   Filename: today.f71
      case 106.  3.600E03 seconds   0.000E00
    total strength:  2.2051E19 gammas/second
    average energy:   0.7865806796307987
    discrete lines:  0.0000E00 gammas/second
                     0.00% of energy
    average line energy:   0.0
    multigroup bins: 2.2051E19 gammas/second
                     100.00% of energy
    average group energy:   0.7865806796307987
    not counted:      1.4098E11 gammas/second
                     0.00% of the original energy
-------------------------------------------------------------


Multigroup bins (in MeV) and their probabilities
    groups: 50  fraction: 1.0
    5.0000E00    4.6645E-09
    4.9000E00    4.1081E-07
    4.8000E00    6.5455E-06
    4.7000E00    9.4904E-09
    4.6000E00    2.5797E-08
    4.5000E00    6.5957E-08
    4.4000E00    3.4599E-08
    4.3000E00    9.0391E-08
    4.2000E00    2.3216E-07
    4.1000E00    4.4053E-05
    4.0000E00    2.5596E-04
    3.9000E00    1.2381E-04
    3.8000E00    2.6967E-04
    3.7000E00    6.5175E-04
    3.6000E00    5.9104E-04
    3.5000E00    3.7149E-04
    3.4000E00    8.9525E-04
    3.3000E00    5.2663E-04
    3.2000E00    1.0270E-03
    3.1000E00    1.1293E-03
    3.0000E00    1.1971E-03
    2.9000E00    1.1819E-03
    2.8000E00    9.7390E-04
    2.7000E00    6.6506E-03
    2.6000E00    6.0077E-03
    2.5000E00    1.7266E-03
    2.4000E00    7.3536E-03
    2.3000E00    1.0536E-02
    2.2000E00    6.7957E-03
    2.1000E00    1.0070E-02
    2.0000E00    5.9813E-03
    1.9000E00    7.1253E-03
    1.8000E00    9.9440E-03
    1.7000E00    1.1682E-02
    1.6000E00    1.3600E-02
    1.5000E00    4.8977E-02
    1.4000E00    2.1962E-02
```

```
1.3000E00    1.6226E-02
1.2000E00    2.2041E-02
1.1000E00    4.2262E-02
1.0000E00    5.3605E-02
9.0000E-01   1.1609E-01
8.0000E-01   5.3579E-02
7.0000E-01   5.3704E-02
6.0000E-01   6.2564E-02
5.0000E-01   8.4903E-02
4.0000E-01   1.2800E-01
3.0000E-01   5.1986E-02
2.0000E-01   8.4751E-02
1.0000E-01   5.2631E-02
0.0000E00
```

90%/10% U-235/U-238 at 1 Hour

 Photon Source Definition - generated from ORIGEN F71 file
   Filename: today.f71
      case 106.   3.600E03 seconds   0.000E00
    total strength: 2.2393E19 gammas/second
    average energy: 0.8220924456853023
    discrete lines: 0.0000E00 gammas/second
                     0.00% of energy
    average line energy: 0.0
    multigroup bins: 2.2393E19 gammas/second
                     100.00% of energy
    average group energy: 0.8220924456853023
    not counted: 5.5186E16 gammas/second
                     1.10% of the original energy

Multigroup bins (in MeV) and their probabilities
     groups: 35   fraction: 1.0
    3.5000E00   3.6600E-04
    3.4000E00   9.5663E-04
    3.3000E00   5.7590E-04
    3.2000E00   6.1879E-04
    3.1000E00   1.1195E-03
    3.0000E00   1.2714E-03
    2.9000E00   1.2060E-03
    2.8000E00   9.2172E-04
    2.7000E00   7.1114E-03
    2.6000E00   8.1765E-03
    2.5000E00   1.9391E-03
    2.4000E00   1.0378E-02
    2.3000E00   1.2126E-02
    2.2000E00   8.8413E-03
    2.1000E00   1.0719E-02
    2.0000E00   5.4976E-03
    1.9000E00   9.5165E-03
    1.8000E00   1.0375E-02
    1.7000E00   8.9979E-03
    1.6000E00   1.3411E-02
    1.5000E00   5.4511E-02
    1.4000E00   3.0795E-02
    1.3000E00   2.0595E-02
    1.2000E00   2.1935E-02
    1.1000E00   5.1278E-02
    1.0000E00   5.5379E-02
    9.0000E-01   1.1571E-01
    8.0000E-01   5.2353E-02
    7.0000E-01   5.1749E-02
    6.0000E-01   5.6240E-02
    5.0000E-01   9.3161E-02
    4.0000E-01   8.4548E-02
    3.0000E-01   5.6112E-02
    2.0000E-01   8.6115E-02
    1.0000E-01   5.5395E-02
    0.0000E00

```
Excerpt of Isotope Contributions of 90%/10% U-235/U-238 at 72 Hours
-------------------------------------------------------------------
 Photon Source Definition - generated from ORIGEN F71 file
   Filename: today.f71
     case 125.  2.592E05 seconds   0.000E00
   total strength:  1.3112E17 gammas/second
   average energy:   0.42279692832610744
   discrete lines:  1.3112E17 gammas/second
                    100.00% of energy
   average line energy:   0.42279692832610744
   multigroup bins: 0.0000E00 gammas/second
                    0.00% of energy
   average group energy:   0.0
   not counted:      0.0000E00 gammas/second
                    0.00% of the original energy
-------------------------------------------------------------------


Discrete lines (in MeV) and their probabilities


    1.5900E00 1.2662E-31 Dy-155
    1.5914E00 8.0662E-08 Sn-125
    1.5918E00 1.3275E-26 Tm-166
    1.5925E00 6.7550E-22 Sr-83
    1.5927E00 4.7924E-19 Ag-110m
    1.5930E00 1.8146E-14 Eu-154
    1.5931E00 3.1148E-05 I-132
    1.5932E00 2.5694E-06 Sb-128
    1.5938E00 2.8235E-14 Pa-234
    1.5945E00 2.4707E-31 Dy-155
    1.5947E00 4.6602E-26 Bi-214
    1.5953E00 6.6337E-20 Ba-139
    1.5960E00 1.7296E-14 Cd-117
    1.5961E00 3.0011E-23 Pr-140
    1.5962E00 2.5568E-02 La-140
    1.5964E00 3.3600E-37 Er-161
    1.5965E00 3.2226E-14 Eu-154
    1.5966E00 8.9195E-28 Pr-139
    1.5967E00 1.4203E-07 Ga-72
    1.5967E00 7.3566E-28 Tm-166
    1.5968E00 1.1032E-24 As-72
    1.5969E00 2.0042E-34 Eu-158
    1.5973E00 3.4591E-14 Cd-117
    1.5976E00 1.5713E-21 Sr-83
    1.5985E00 1.8830E-26 As-71
    1.5985E00 2.5184E-08 Sb-129
    1.5993E00 5.8683E-26 Bi-214
    1.5996E00 1.1983E-30 Dy-155
    1.6000E00 1.7528E-14 Sn-127
```

```
Excerpt of Isotope Contributions of 90%/10% U-235/U-238 at 1 Month
-------------------------------------------------------------------
 Photon Source Definition - generated from ORIGEN F71 file
   Filename: today.f71
     case 137.  2.630E06 seconds   0.000E00
   total strength:  7.2408E15 gammas/second
   average energy:   0.629771890136701
   discrete lines:  7.2408E15 gammas/second
                    100.00% of energy
   average line energy:   0.629771890136701
   multigroup bins: 0.0000E00 gammas/second
                    0.00% of energy
   average group energy:   0.0
   not counted:      0.0000E00 gammas/second
                    0.00% of the original energy
-------------------------------------------------------------------


Discrete lines (in MeV) and their probabilities

    1.5841E00 5.4932E-24 Lu-172
    1.5854E00 2.6928E-13 Pa-234
    1.5882E00 3.1849E-21 Ac-228
    1.5899E00 1.0086E-14 I-133
    1.5914E00 2.0312E-07 Sn-125
    1.5925E00 9.3175E-27 Sr-83
    1.5927E00 8.0421E-18 Ag-110m
    1.5930E00 3.2662E-13 Eu-154
    1.5931E00 1.4908E-06 I-132
    1.5932E00 4.6439E-27 Sb-128
    1.5938E00 6.4627E-13 Pa-234
    1.5947E00 4.0811E-22 Bi-214
    1.5961E00 1.9242E-24 Pr-140
    1.5962E00 1.5807E-01 La-140
    1.5965E00 5.8004E-13 Eu-154
    1.5967E00 1.5376E-10 Ga-72
    1.5968E00 3.8346E-29 As-72
    1.5976E00 2.1673E-26 Sr-83
    1.5985E00 3.1341E-28 As-71
    1.5993E00 5.1390E-22 Bi-214
```

A p p e n d i x   D

Weighted Average Build Up Factor Data for 90/10 U-235 at One Hour

Incident Energy (MeV)	Post-Scatter Energy (MeV)	% Air Contribution Above Detector	% Air Contribution Below Detector	% Contribution from Air Scatter (Isotropic)	% Contribution from Ground Scatter (Isotropic)	% Total Contribution 2nd Flight (Isotropic)	GNAT	Weight	BUF	SNC (J-m^2 /kg/sec/Bq)
0.020	0.019	61.86%	38.14%	35.26%	1.58%	36.84%	0.46	0.11	1.463	3.6186E-16
0.030	0.028	69.98%	30.02%	26.55%	3.69%	30.24%	0.44	0.36	1.375	1.6419E-16
0.040	0.037	72.97%	27.03%	22.81%	6.05%	28.86%	0.43	0.27	1.341	9.952E-17
0.050	0.046	74.35%	25.65%	20.67%	7.98%	28.65%	0.41	0.04	1.319	7.515E-17
0.060	0.054	75.16%	24.84%	18.90%	9.13%	28.03%	0.39	0.01	1.298	6.6817E-17
0.070	0.062	75.70%	24.30%	17.67%	9.69%	27.36%	0.38	0.00	1.281	6.6291E-17
0.080	0.070	76.13%	23.87%	16.61%	10.04%	26.65%	0.37	0.19	1.265	6.9925E-17
0.090	0.078	76.48%	23.52%	15.89%	10.20%	26.09%	0.35	0.02	1.252	7.5976E-17
0.100	0.086	76.79%	23.21%	15.30%	10.28%	25.58%	0.34	0.01	1.241	8.3765E-17
0.200	0.153	78.86%	21.14%	12.20%	9.35%	21.55%	0.25	0.10	1.177	1.8911E-16
0.300	0.211	80.16%	19.84%	10.74%	8.47%	19.21%	0.20	0.06	1.147	3.0781E-16
0.400	0.260	81.10%	18.90%	9.62%	7.70%	17.32%	0.16	0.10	1.126	4.1981E-16
0.500	0.305	81.84%	18.16%	8.77%	7.10%	15.87%	0.13	0.11	1.111	5.3146E-16
0.600	0.344	82.55%	17.45%	8.10%	6.53%	14.63%	0.11	0.06	1.100	6.4279E-16
0.700	0.380	82.96%	17.04%	7.48%	6.14%	13.62%	0.10	0.06	1.090	7.4302E-16
0.800	0.413	83.39%	16.61%	6.95%	5.73%	12.67%	0.09	0.06	1.083	8.5302E-16
0.900	0.444	83.78%	16.22%	6.51%	5.39%	11.90%	0.08	0.13	1.076	9.3949E-16
1.000	0.472	84.21%	15.79%	6.18%	5.09%	11.26%	0.07	0.06	1.072	1.0327E-15
1.100	0.499	84.41%	15.59%	5.77%	4.81%	10.58%	0.06	0.06	1.066	1.1209E-15
1.200	0.524	84.68%	15.32%	5.46%	4.57%	10.03%	0.06	0.02	1.062	1.2075E-15
1.300	0.547	84.94%	15.06%	5.17%	4.34%	9.51%	0.05	0.02	1.059	1.2913E-15
1.400	0.569	85.18%	14.82%	4.92%	4.13%	9.05%	0.05	0.03	1.055	1.3736E-15
1.500	0.590	85.39%	14.61%	4.70%	3.94%	8.64%	0.05	0.06	1.052	1.4527E-15
1.600	0.610	85.59%	14.41%	4.48%	3.77%	8.25%	0.04	0.02	1.050	1.5289E-15
1.700	0.629	85.77%	14.23%	4.29%	3.61%	7.90%	0.04	0.01	1.047	1.6027E-15
1.800	0.647	85.94%	14.06%	4.12%	3.46%	7.57%	0.04	0.01	1.045	1.6744E-15
1.900	0.665	86.10%	13.90%	3.96%	3.32%	7.28%	0.03	0.01	1.043	1.7439E-15
2.000	0.682	86.25%	13.75%	3.81%	3.20%	7.01%	0.03	0.01	1.041	1.8117E-15
2.500	0.757	86.90%	13.11%	3.21%	2.66%	5.87%	0.03	0.00	1.034	2.1275E-15
3.000	0.822	87.39%	12.61%	2.77%	2.28%	5.05%	0.02	0.00	1.029	2.4073E-15
3.500	0.878	87.80%	12.20%	2.44%	1.97%	4.41%	0.02	0.00	1.026	2.6601E-15

Weight Values From the ORIGEN Fallout Analysis Tool for 90/10 U-235 at 12 hours

Incident Energy (MeV)	BUF	Weight
0.020	1.463	
0.030	1.375	
0.040	1.341	
0.050	1.319	
0.060	1.298	6.64E-02
0.070	1.281	
0.080	1.265	
0.090	1.252	
0.100	1.241	
0.200	1.177	5.08E-02
0.300	1.147	1.65E-01
0.400	1.126	2.61E-02
0.500	1.111	2.27E-02
0.600	1.100	1.57E-01
0.700	1.090	1.49E-01
0.800	1.083	8.00E-02
0.900	1.076	3.41E-02
1.000	1.072	3.59E-02
1.100	1.066	4.33E-02
1.200	1.062	3.52E-02
1.300	1.059	3.64E-02
1.400	1.055	3.77E-02
1.500	1.052	1.68E-02
1.600	1.050	7.33E-03
1.700	1.047	1.06E-02
1.800	1.045	1.39E-02
1.900	1.043	7.02E-03
2.000	1.041	2.50E-03
2.500	1.034	1.10E-03
3.000	1.029	2.15E-04
3.500	1.026	7.40E-05

12 Hour Case Sample Calculations

Avg BUF:	1.12E+00	
Avg Energy:	6.93E-01	MeV
Total Activity:	8.00E+17	ph/sec

Avg Energy Predicted SNC Value:	7.49E-16
WW Predicted Activity Value:	1.13511E+18

Bibliography

1. Bridgman, Charles J. *Introduction to the Physics of Nuclear Weapons Effects.* DTRA, 2001.

2. Baum, Edward M., Harold D. Knox and Thomas R. Miller. *Nuclides and Isotopes.* KAPL Inc. Sixteenth Edition, 2002.

3. Evans, Robley D. *The Atomic Nucleus.* Krieger Publishing Company, 1955.

4. Glasstone, Samuel and Philip Dolan. *The Effects of Nuclear Weapons.* Washington, DC: U.S. Government Printing Office, Third Edition, 1977.

5. Herte, Mark S. *The Self-Shielding of Fallout Gamma Rays by Terrain Roughness.* Thesis, AFIT/GNE/ENP/91M-2. Wright-Patterson AFB, OH: Graduate School of Engineering, Air Force Institute of Technology. July 1991 (91-05727).

6. Jodoin, Vincent J. *Nuclear Cloud Rise and Growth.* Ph.D. dissertation, AFIT/DS/ENP/94J-2. Wright-Patterson AFB, OH: Graduate School of Engineering, Air Force Institute of Technology. June 1994 (AD-A280688).

7. Jodoin, Vincent J., Ronald W. Lee, Douglas E. Peplow and Jordan P. Lefebvre. "Application of the ORIGEN Fallout Analysis Tool and the DELFIC Fallout Planning Tool to National Technical Nuclear Forensics," *11th Emergency Preparedness & Response.* American Nuclear Society, LaGrange Park, IL, 2011.

8. Pugh, George E. and Robert J. Galiano. *An Analytical Model of Close-In Deposition of Fallout for Use in Operational Type Studies.* WESG Research Memorandum No 10. Washington, DC: The Pentagon, Weapon System Evaluation. October 15, 1959 (AD 261752).

9. Way, Katherine and E.P. Wigner. "The Rate of Decay of Fission Products." *Physical Review.* Vol. 76:375. 1948.

10. XCOM: Photon Cross Sections Database. November 2010 Version 3.1. National Institute of Standards and Technology. 10 June 2010.
http://www.nist.gov/pml/data/xcom/index.cfm

1. REPORT DATE *(DD-MM-YYYY)*	**2. REPORT TYPE**	**3. DATES COVERED** *(From – To)*
15092011	Master's Thesis	Aug 2009-Sep 2011

4. TITLE AND SUBTITLE	**5a. CONTRACT NUMBER**
Source Normalization Constants for Ground Distributed Fallout Fields	
	5b. GRANT NUMBER
	5c. PROGRAM ELEMENT NUMBER

6. AUTHOR(S)	**5d. PROJECT NUMBER**
Smith, Justin M, Capt, USAF	
	5e. TASK NUMBER
	5f. WORK UNIT NUMBER

7. PERFORMING ORGANIZATION NAMES(S) AND ADDRESS(S)	**8. PERFORMING ORGANIZATION REPORT NUMBER**
Air Force Institute of Technology	
Graduate School of Engineering and Management (AFIT/EN)	
2950 Hobson Way	AFIT/GNE/ENP/11S02
Wright-Patterson AFB OH 45433-7765	

9. SPONSORING/MONITORING AGENCY NAME(S) AND ADDRESS(ES)	**10. SPONSOR/MONITOR'S ACRONYM(S)**
Domestic Nuclear Detection Office	
Department of Homeland Security	DNDO
Washington, DC 20528	**11. SPONSOR/MONITOR'S REPORT NUMBER(S)**
ATTN: DNDO	
dndo.info@dhs.gov	

12. DISTRIBUTION/AVAILABILITY STATEMENT
Distribution Statement A: Approved for public release; distribution is unlimited

13. SUPPLEMENTARY NOTES

14. ABSTRACT
Five assumptions regarding a first order model developed to calculate dose rate at a detector above a fallout field are analyzed. The omission of scattering is relaxed by the method of successive scatters resulting in a build up factor of 1.1. The use of a single average photon energy to represent a fallout distribution is analyzed using the Oak Ridge National Laboratory Isotope Generator (ORIGEN) Fallout Analysis Tool. An average photon energy of 0.81MeV is calculated and shown to be an accurate approximation of the fallout field energy distribution. A Gaussian distribution is used to calculate the minimal impact of non-uniform activity density on the source normalization constant (SNC). The effects of time on the SNC are also examined by the ORIGEN Fallout Analysis Tool and shown to warrant an additional time correction factor. Finally, previous research accomplished by Herte reveals 2-5% self-shielding from terrain roughness. These findings are incorporated into an updated SNC value that is 25% greater than the value found from the first order model.

15. SUBJECT TERMS
Dose Conversion Factor, Source Normalization Constant, Dose Rate, Fallout Field

16. SECURITY CLASSIFICATION OF:			**17. LIMITATION OF ABSTRACT**	**18. NUMBER OF PAGES**	**19a. NAME OF RESPONSIBLE PERSON**
					Dr. Charles J. Bridgman
REPORT U	**ABSTRACT** U	**c. THIS PAGE** U	UU	89	**19b. TELEPHONE NUMBER** *(Include area code)* (937) 255-3636 x4679